NBER WORKING PAPER SERIES

COOL CITIES: THE VALUE OF URBAN TREES

Lu Han
Stephan Heblich
Christopher Timmins
Yanos Zylberberg

Working Paper 32063
http://www.nber.org/papers/w32063

NATIONAL BUREAU OF ECONOMIC RESEARCH
1050 Massachusetts Avenue
Cambridge, MA 02138
January 2024

We did not receive external funding for this research. Lu Han gratefully acknowledges financial support from the Social Sciences and Humanities Research Council of Canada. We would like to thank Piet Eichholtz, Pierre-Philippe Combes, Naomi Hausman, Matthew Kahn, Giacomo Ponzetto, Yu Qin, Stuart Rosenthal, Stijn Van Nieuwerburgh, John Yinger, and Siqi Zheng as well as seminar audiences at ABFER, Bristol, the NBER Summer Institute, the Syracuse Urban Economics Workshop, and UEA for helpful comments. The usual disclaimer applies. The views expressed herein are those of the authors and do not necessarily reflect the views of the National Bureau of Economic Research.

Cool cities: The value of urban trees
Lu Han, Stephan Heblich, Christopher Timmins, and Yanos Zylberberg
NBER Working Paper No. 32063
January 2024
JEL No. Q4,Q51,Q54,R3

ABSTRACT

This paper estimates the value of urban trees. The empirical strategy exploits an ecological catastrophe — the Emerald Ash Borer (EAB) infestation in Toronto to isolate exogenous variation in neighborhood tree canopy changes. Adding one tree to a postcode increases property prices by 0.40%; the hardest-hit areas lost 7% tree cover, resulting in a 6% property price decline. The tree premium includes the value of tree services and aesthetics. Our results demonstrate a significant impact of trees on mitigating urban heat and generating energy savings. However, the total amenity value of trees exceeds the combined value of these services.

Lu Han
Wisconsin School of Business
975 University Ave
Madison, WI 53711
lu.han@wisc.edu

Stephan Heblich
Munk School of Global Affairs
and Public Policy
University of Toronto
1 Devonshire Place
Toronto, ON M5S 3K7
and NBER
stephan.heblich@utoronto.ca

Christopher Timmins
Real Estate and Urban Land Economics
Wisconsin School of Business
4291 Grainger Hall
975 University Avenue
Madison, WI 53706
and NBER
ctimmins@wisc.edu

Yanos Zylberberg
University of Bristol
8 Woodland Road
Bristol BS8 1TN
UK
yanos.zylberberg@bristol.ac.uk

Since 2002, the invasive Emerald Ash Borer beetle has affected millions of trees in North America, including a significant portion of urban trees. This ecological catastrophe has underscored the social value of green capital in cities. Urban forestry enhances aesthetics (Benson et al., 1998; Price, 2003; Todorova et al., 2004), but trees also provide a variety of important services (Willis and Petrokofsky, 2017; Manning et al., 2023). For instance, studies have shown positive health effects (Kardan et al., 2015), and trees reduce noise (Kragh, 1981), improve local air quality (Nowak et al., 2006; Jones and McDermott, 2018b), provide wind-sheltering (Akbari and Taha, 1992), help manage storm-water runoff (Rahman et al., 2023), and act as a store of carbon (Pennisi, 2019; Hubau et al., 2020; Gatti et al., 2023; Barham et al., 2023; Deshmukh et al., 2023; Tucker et al., 2023). Finally, the cooling benefits offered by the tree canopy via evapotranspiration and shading alleviate *urban heat island* effects, a climatic hazard to urban residents (Iungman et al., 2023; Hajat and Kosatky, 2010).[1]

This paper aims to quantify the value of urban forestry. The empirical strategy relies on the Emerald Ash Borer (EAB) infestation and its large, yet heterogeneous, impact on urban forestry across neighborhoods in North-American cities.[2] The Emerald Ash Borer exclusively feeds on ash trees, one of the most common species in New York, Chicago or Toronto. For instance, the City of Toronto (rightly) expected to lose nearly all of its 860,000 ash trees within ten years after the first signs of infestation around 2007; this amounts to about 8% of the tree canopy cover over both public and private land, with very significant variation within and across neighborhoods.[3] We rely on comprehensive urban forest assessments covering

[1]The *urban heat island* effect will affect a rapidly increasing share of the World population because of climate change and the swift growth of large, densely-populated urban settlements in developing economies (Tuholske et al., 2021). Earlier contributions have identified urban forestry as an important mitigating factor (Peng et al., 2012), especially so in dry climates (Manoli et al., 2019). The unequal distribution of urban forestry and built-up surfaces within urban settlements thus induces large inequalities in exposure to extreme heat episodes (Hsu et al., 2021): Affluent, greener neighborhoods experience more moderate temperature peaks during periods of extreme heat.

[2]The Emerald Ash Borer, originally native to Asia, was inadvertently introduced to North America during the summer of 2002. Since that fateful introduction, it has emerged as one of the most devastating non-native insect species in North America. As of 2018, its destructive reach extended across 33 U.S. states and the Canadian provinces of Ontario, Quebec, and Manitoba, resulting in the demise of hundreds of millions of ash trees (Aukema et al., 2011; Herms and McCullough, 2014). The ash borer was recently reported in Oregon, its first appearance west of the rocky mountains (Popkin, 2022). Live updates are provided by the Emerald Ash Borer Network.

[3]The previous infestation of such amplitude was the Dutch elm disease, spreading from 1940 to 1970 in North America. Interestingly, this catastrophe shaped the subsequent impact of the EAB infestation: urban planners often decided to replace the infested elm trees—the first-best urban tree—with ash trees. In Toronto, city-managed trees are predominantly from a few selected species, e.g., maple trees, elm trees, ash trees, or linden trees, selected for their resistance to climatic and

Toronto in 2007 and 2018 to evaluate local changes in the tree canopy, and we use a geo-referenced register of all city-managed urban trees, which reports tree species, maintenance dates, and cut downs, to isolate exposure to the EAB infestation within each of 45,000 postal codes.[4]

We begin by assessing the hedonic value of the urban tree canopy, employing exhaustive data on residential property transactions between 2007 and 2017. The key challenge lies in establishing a causal link between tree canopies and house prices. One may be concerned that leafy neighborhoods might also enjoy unobserved amenities like superior school quality, which would bias the correlation between tree density and property values upward. Conversely, in highly sought-after, densely populated neighborhoods, the opportunity cost of land may be greater, potentially causing a downward bias. To mitigate these concerns and establish causality, we employ an instrumental variable approach and instrument the evolution of the tree canopy within a postal code by its exposure to the EAB infestation. We find that one additional tree within a postcode increases property prices by 0.40%; alternatively, one additional percentage point in tree cover within a postcode elevates property values by 0.86%. Neighborhoods where ash trees constituted the majority of city-managed trees prior to the infestation witnessed a staggering 7 percentage point reduction in tree cover, corresponding to a 6% drop in property prices.

Next, we aim to quantify the role of one specific tree service—energy savings—in explaining the "tree premium." Heatwaves trigger spikes in energy consumption, and these surges are mitigated in neighborhoods with a generous tree canopy. Our analysis reveals that one additional percentage point of tree cover within a postal code area results in a 0.05-degree Celsius reduction in the local *average* Land Surface Temperature (LST) during the months of July and August. This decrease in temperature translates into a reduction in energy consumption of roughly 2.5%, corresponding to a monthly cost saving of CAD 5 during this two-month period. We utilize these estimates to place a monetary value on the role of trees in alleviating urban heat island effects under varying scenarios, encompassing more and less con-

hostile urban conditions. There is significant spatial clustering in the local composition of street-managed trees such that some neighborhoods would mostly be populated by elm trees or maple trees (and thus spared by the recent infestation), when others would predominantly feature ash trees.

[4]The 2007 land cover data was part of the "Urban Tree Canopy (UTC) Assessment" conducted by the City of Toronto and summarized in "Every Tree Counts: A Portrait of Toronto's Urban Forest"; the later update was titled the "2018 Tree Canopy Study". Both assessments were based on high-quality satellite imagery, LiDAR information, and manual corrections. We complement these two highly-precise cross-sections with yearly vegetation indices constructed from satellite imagery (Sentinel 2, 2016–2020, Landsat L8, 2013–2020, Landsat L7, 2006–2012) to document the swift, persistent loss of tree canopy between 2012–2016 with little evidence of any reversion in the medium run.

servative climate change projections. Our findings reveal substantial energy savings attributed to urban trees. The monetary value of this one tree service already exceeds the annual maintenance costs per tree. Yet, this is but a portion of the total hedonic value associated with trees. This underscores that urban trees provide a cost-effective way to regulate temperatures in urban areas.

While urban forests are widely recognized for their amenity value, urban development plans that involve densification and sprawl may not consistently incorporate this value, paradoxically leading to a reduction in tree canopies (Nowak and Greenfield, 2012, 2018). A specific concern arises from the potential exacerbation of the existing inequality in tree canopy cover between economically disadvantaged and affluent neighborhoods. Our study offers a plausible explanation for why such a phenomenon could occur: the presence of non-linearities in the valuation of urban forestry, coupled with coordination failures. In line with this, we observe that the marginal value of a tree becomes more pronounced in neighborhoods with substantial existing tree cover. This finding underscores the need for policy interventions targeting cities or neighborhoods with limited green infrastructure. Public provision of green space could yield positive outcomes by enhancing the returns on further green policies or subsequent private investments, such as those in new residential developments or private gardens.

Our identification strategy hinges on the assumption that the spatial distribution of ash trees is exogenous to the dynamics of residential prices and energy consumption across postal codes. We offer support for this hypothesis through several avenues. First, we condition the analysis on (i) the density of all city-managed trees, (ii) ward fixed-effects, and (iii) 8 categories of 2007 land cover, interacted with year fixed-effects. Second, we demonstrate that changes in the evolution of the tree canopy between 2007 and 2018 can be predominantly attributed to variations in the local density of ash trees rather than other tree species. Third, we show that there are no differential dynamics in property prices before our baseline period (i.e., between 2002 and 2006). Fourth, although our main empirical framework leverages the EAB infestation as an ecological catastrophe to isolate substantial shifts in tree cover, we also leverage fluctuations in extreme weather episodes, interacted with the positioning of trees around each property, to understand their potential to save energy.[5]

[5] More precisely, we calculate the *solar-shading potential* and *wind-sheltering potential* of each tree in each month of the year, by combining the relative positioning of the tree and the property with solar angles and monthly wind roses across the year (as in Nikoofard et al., 2011; Upreti et al., 2017). The annual average of these measures may be correlated with general levels of energy consumption, as positions of trees might partly reflect optimization behavior from households. The identifying assumption is that excess energy savings during extreme weather episodes are

The main contribution of this paper is to provide causal estimates for the amenity value of urban forests and to isolate one increasingly important tree service: their ability to mitigate temperature increases during heat waves. This paper is not the first one to estimate the hedonic price of urban forestry (see, e.g., Morales, 1980; Wachter and Wong, 2008; Conway et al., 2010; Franco and Macdonald, 2018), or its effect on temperature during heat waves and on energy savings (see, e.g., Akbari and Taha, 1992; Nikoofard et al., 2011). These previous attempts however suffer from omitted variation and reverse causation. An exception to this is Druckenmiller (2023), which exploits differences in temperatures across the American West, creating conditions that are more or less conducive to the survival of bark beetles. In contrast to our approach, this study centers on forests in a broader sense, while our research specifically delves into the distinct role of urban forestry.

Our research relates to different strands of the literature. First, it contributes to research at the intersection of urban and environmental economics which assesses the value of green urban infrastructure. The (monetary) value of trees has been widely recognized by urban planners and Mullaney et al. (2015) provide a comprehensive review of this literature.[6] Druckenmiller (2022) highlights the challenges in measuring the value of tree cover and ecosystem services more broadly for use in climate change policy. We contribute to this literature by leveraging exogenous variation and providing causal estimates of the amenity value of trees. Secondly, we leverage our source of exogenous variation to gauge the capacity of the tree canopy to curtail energy consumption during periods of extreme heat. This part relates to Auffhammer (2018) who assesses how future climate change will affect energy consumption in California, and to research on the value of green buildings (Eichholtz et al., 2010, 2013) and energy-efficient houses (as reviewed in Kahn and Walsh, 2015). Lastly, we add to the literature on the effects of climate change on densely populated urban areas (see, for instance, the review articles by Dell et al., 2014; Graff Zivin and Neidell, 2013; Kahn and Walsh, 2015). Indeed, urbanization comes with a concentration of impervious surfaces like stone, concrete and asphalt, at the expense of vegetation. The resulting temperature differentials between urban areas and the adjacent countryside, the *urban heat island* effect (Oke, 1973), raises energy

not directly correlated with either the *solar-shading potential* or the *wind-sheltering potential*—other than through the mitigation effect of trees themselves. Using panel data on residential electricity meter readings at the postcode/month level from 2011–2021 and natural gas data at the postcode/month level from 2010–2017, we show that the tree canopy substantially affects the elasticity of energy consumption to heat waves and episodes of wind chill (to a lesser extent).

[6] Jones and McDermott (2018a) point out that most papers focus on the benefits of trees without consideration of costs. To address this, they develop a bio-economic health model that accounts for a range of benefits, costs and externalities and calibrate it to data from New York City. They report positive, yet smaller, net benefits of trees than commonly reported in the literature.

demand for cooling (an effect expected to worsen in the presence of climate change, see Santamouris et al., 2015; Estrada et al., 2017). One way to mitigate urban heat island effects is to invest in the urban canopy (Bowler et al., 2010; Roy et al., 2012). We contribute to this literature by providing more direct and granular evidence of the effect of urban forestry on household energy consumption.

The remainder of the paper is structured as follows. In Section 1, we describe the context, the data sources and the effect of the Emerald Ash Borer infestation on urban forestry. Section 2 presents the empirical strategy. Sections 3 and 4 provide causal estimates of the hedonic price of urban forestry and its effect on urban heat and energy savings. The final section concludes.

1 Context, data and evolution of the tree canopy

This section discusses the allocation of ash trees across neighborhoods of Toronto and the evolution of the Emerald Ash Borer (EAB) infestation since 2007. We then describe our data sources and data construction. We finally shed light on the relationship between the EAB infestation and the evolution of the tree canopy, which constitutes the first stage of our baseline empirical strategy.

1.1 Context

Toronto is one of the greenest cities in North America. The 2018 Tree Canopy Study found that Toronto has an estimated 11.5 million trees, as much as the combined number of trees in New York (5.2 million) and Los Angeles (6 million).[7] The tree population in Toronto consists of a large number of native trees, which date back to the Carolinian forests before the 18th century. These species include: black, green and white ash; birch; white cedar; American chestnut; white elm; maple; black, red, white oak; white pine, etc. Additional non-native species were introduced by European settlers, e.g., barberry, larch, lilac, Norway maple or pine.

Dutch elm disease and the allocation of trees before 2007 Growing trees in cities is notoriously difficult. Road salt, compact soil, pollution and Canada's winters all make urban areas of Toronto unkind to trees. The tree of choice in such harsh environments used to be elm trees, which thrive in urban areas and present

[7] Apart from the Central Business District and industrial parks, most neighborhoods have alleys of trees or public parks.; and houses in rich residential neighborhoods have backyard gardens with significant tree coverage. The City of Toronto estimates that the structural value of its urban forest amounts to CAD 7 billion, with ecosystem services worth more than CAD 55 million each year (City of Toronto, 2019).

convenient aesthetic features. Elm trees were primarily planted at the beginning of the 20th century in North America, such that their allocation across the city of Toronto coincides with neighborhood growth between 1900 and 1930.

Elm trees steadily disappeared from most North-American cities due to the Dutch elm disease. Around 1930, elm bark beetles appeared in New York, carrying the Dutch elm disease and threatening the large population of trees in New Haven. However, the disease did not start to propagate until the Second World War when the quarantine and sanitation procedures that had been implemented since 1928 were abandoned due to budget restrictions. After the Dutch elm disease swept through toward the second half of the last century, most municipalities planted ash trees as a "second-best" urban tree (MacFarlane and Meyer, 2005). The more recent allocation of ash trees thus closely relates to the past allocation of elm trees across and within cities of the East Coast. Neighborhoods of Toronto with large populations of elm trees in 1930, e.g., Scarborough or Mount Pleasant, had a large population of ash trees until very recently.

Emerald Ash Borer infestation The Emerald Ash Borer is a beetle that was accidentally introduced to North America around 2000. This invasive species survives well in the North American environment, due to a lack of natural predators. The beetle attacks ash trees at all stages of its life-cycle: the larva feeds aggressively on tissues, which produces larval galleries and frass; the young adult escapes the tree, leaving holes in the bark—one of the first recognizable symptoms of infestation; and the full-grown beetle then feeds on ash foliage and would lay clusters of eggs in crevices of the bark. Accordingly, infested trees present bark fissures, larval galleries, high woodpecker activity (feeding on borers), and yellow foliage. Without specific treatment at the very early stages of the infestation, e.g., TreeAzin injections, it takes between 1 and 4 years for an infested ash tree to die.[8] Between 2007 and 2018, the City of Toronto had lost a majority of its ash trees.[9]

1.2 Data sources

This section presents the data sources used in this research.

[8]Alternative efforts to protect the ash tree population through selective breeding have been undertaken as well (Popkin, 2022).

[9]Removals were concentrated in Scarborough, North York and Etobicoke. Trees in Downtown Toronto received early TreeAzin injections, possibly delaying or preventing their full infestation. To address this possible issue, our instrument will use an Intention-To-Treat (ITT) approach and leverage the initial density of ash trees, rather than the actual removal of infested trees.

Figure 1. Land use classification in 2007 and (city-managed) ash trees.

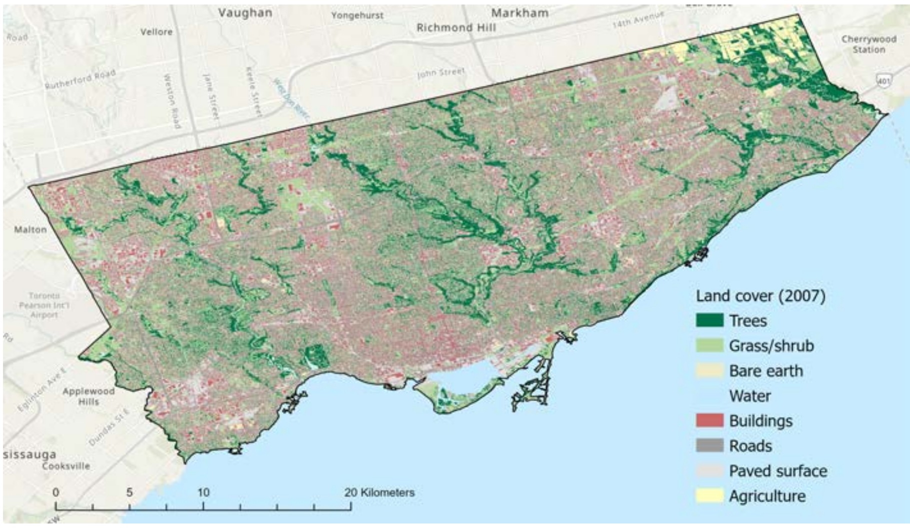

(a) Land use (2007)

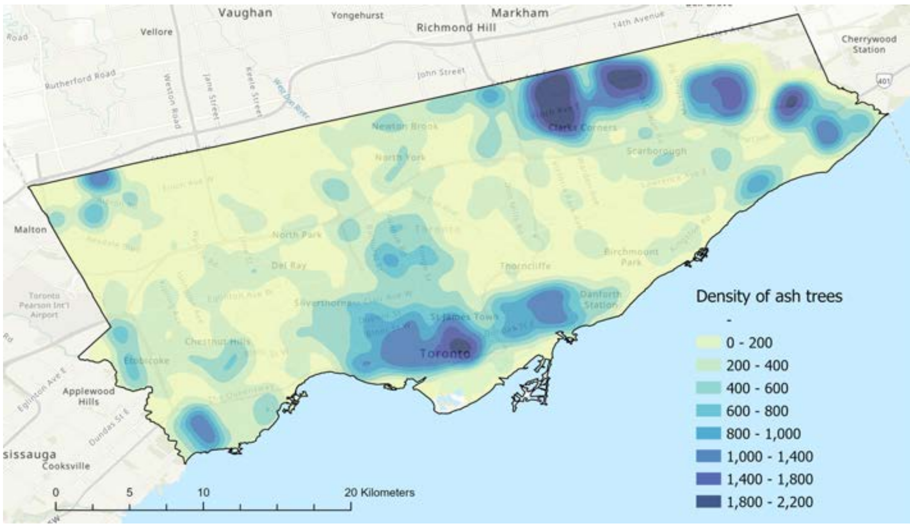

(b) City-managed ash trees

Notes: Panel (a) displays land use as produced by the Urban Tree Canopy (UTC) Assessment in 2007. Land use is divided into 8 categories: tree canopy (dark green), grass/shrub (lighter green), bare earth (sand), water (blue), buildings (red), roads (dark gray), other paved surfaces (light gray) and agriculture (yellow). Panel (b) shows the local density of city-managed ash trees, across 8 bins of density. Except for the central area, the neighborhoods of Scarborough (East), Mount Pleasant, North York and Etobicoke are the ones with the highest concentration of (city-managed) ash trees.

Tree canopy and land cover To estimate the tree cover and its evolution, we use high-resolution land cover classifications in 2007 and in 2018. These land classifications were conducted by the Urban Forestry services of the City of Toronto using a combination of multispectral QuickBird satellite imagery at a resolution of 0.6m, LiDAR information, and manual corrections (City of Toronto, 2019). The land classifications isolate the following eight categories: tree canopy, grass, bare earth, water, buildings, roads, other paved surfaces, and agriculture. Panel (a) of Figure 1 provides an illustration of land usage across the City of Toronto in 2007. We combine the land classifications in 2007 and 2018 with the delineations of postcodes to construct the area shares of all categories within the different postcodes.[10]

While the city aimed at harmonizing the classification techniques in 2007 and 2018, there may still be measurement error in the assessed evolution of the tree canopy. Our main empirical strategy, based on a two-stage specification, should correct for the possible attenuation bias associated with classification errors—at least to some extent. We complement and validate these measures of land cover with vegetation and built-up indices constructed between 2007 and 2018 from lower-resolution, high-frequency satellite imagery (Sentinel 2, 2016–2020, Landsat L8, 2013–2020, Landsat L7, 2007–2012). We describe the construction of these indices and a few validation exercises in Appendix A.1 and shed some light on the evolution of the tree canopy in Appendix A.2.

Ash trees To identify the location of ash trees, we rely on the register of all publicly maintained street trees provided by the City of Toronto in 2010 (with about 600,000 trees in total, and more than 45,000 ash trees). The data contains the street address, the common tree species and the diameter at breast height, which can be used to infer the crown size. For the latter, we rely on estimates of the relationship between the crown diameter and stem diameter to approximate the area that the crown covers (Hemery et al., 2005; Peper et al., 2014). An additional register focuses on the sub-population of ash trees and on the activity related to the EAB infestation, i.e., the dates of EAB removals and TreeAzin injections. Panel (b) of Figure 1 shows the distribution of city-maintained ash trees across the wider City of Toronto. While ash trees are present in every ward, they are most concentrated in the North-East of the city.

Property values We use exhaustive property transaction data between 2007 and 2017 in order to estimate the hedonic value of the local tree canopy. The data comes with a wide range of transaction and property attributes: the transaction date; price; type of property (35 categories); number of floors; number of bedrooms, kitchens, washrooms, family rooms, and fireplaces; the size of the lot; and parking space. The dataset contains about 387,000 transactions (between 30,000-40,000 per year). To

[10] We use a buffer of 10m around each postal code in the baseline specification to properly capture street trees in front of houses. Further, to facilitate the calculations of the solar-shading or wind-sheltering potential (see Section 4 and Appendix C), we transform the "tree cover" surface into a discrete number of individual trees. More specifically, we construct synthetic trunk locations by randomizing tree trunks every 10 meters inside the "tree coverage" surface.

geolocate properties, we combine the transaction data with a geolocated address register provided by the City of Toronto, and perform a fuzzy string matching algorithm on addresses. Appendix Figure A5 shows the distribution of transactions and their average price across the City of Toronto between 2007 and 2017. In order to correct for the over-representation of transactions in certain neighborhoods, e.g., downtown Toronto or York, the main empirical strategy will weigh each transaction such as to equalize the overall contribution of each postal code.[11]

Energy consumption, temperature, and pollution We gained access to data from all residential electricity meters in the City of Toronto. About 800,000 customer IDs i are nested within 21,000 postcodes p over the period 2012–2020, from which we extract monthly consumption for the median household within a postal code. We also collect monthly data on the aggregate consumption of natural gas per postcode over the period 2010 to 2017; we divide the total gas consumption in a year by the number of registered gas meters to derive a measure of average household gas consumption.[12]

Finally, we collect the Land Surface Temperature (LST) for the months of July and August for each year between 2006 and 2018 using the Thermal Infrared (TIRS) band provided by Landsat L7 (2006–2012) and L8 (2013–2018). Specifically, we calculate the Top of Atmosphere (TOA) Reflectance, convert this brightness measure into a temperature measure, correct for Land Surface Emissivity (LSE) and collapse the measure at the level of postcodes in a given year, T_{pt}. Note that the LSE employs a fractional vegetation measure that is based on the Normalized Difference Vegetation Index (NDVI, see Ermida et al., 2020, for more details). While the LSE correction might induce some mechanical correlation with the presence of trees, this procedure is one of the current state-of-the-art techniques to capture surface temperature at a fine spatial scale with limited in situ measurements (Li et al., 2023), and the induced bias would be an order of magnitude smaller than our estimates. We also rely on Van Donkelaar et al. (2021) to nest monthly estimates of fine particulate matter (PM2.5) across postal codes from 2007 to 2018.

[11] We complement the transaction data with neighborhood characteristics from the cadastre of the City of Toronto that includes detailed information about green spaces, protected ravines, property boundaries, building footprints, the general urban infrastructure, and school locations. We employ this cartographic information to calculate distance to amenities and other controls capturing neighborhood quality.

[12] There are important seasonal patterns in energy consumption. We describe these patterns in Appendix A.5, in which we also discuss the construction of harmonized energy consumption measures at the postcode level.

Figure 2. Ash trees and the evolution of the tree canopy—an illustration.

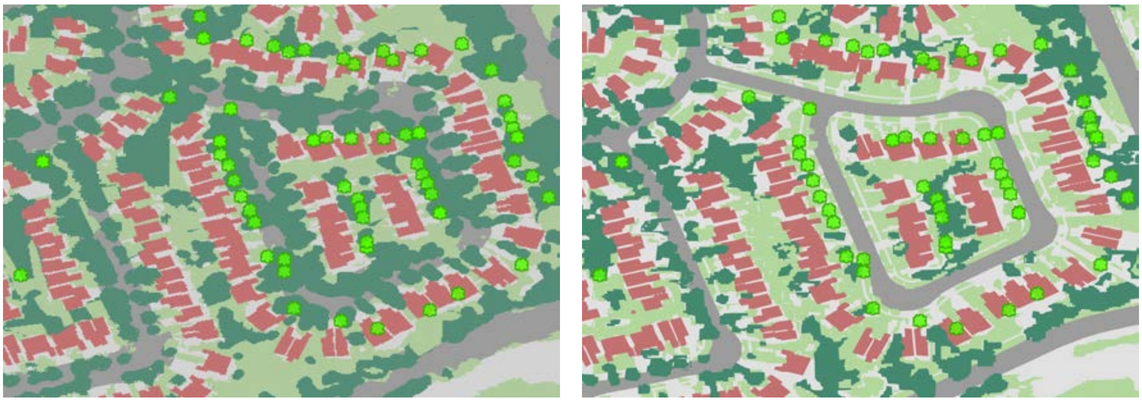

(a) Tree canopy (2007) (b) Tree canopy (2018)

Notes: This Figure shows the land use classification in a given neighborhood in the North-East of Toronto (James Park Square, Scarborough)—with a relatively high density of ash trees. The data was produced in 2007 (left panel) and 2018 (right panel) by Urban Forestry as part of an Urban Tree Canopy (UTC) Assessment. Land cover is represented by the following classes: tree canopy (dark green), grass/shrub (lighter green), bare earth (sand), water (dark blue), buildings (red), roads (dark gray), other paved surfaces (light gray) and agriculture (yellow). The green symbols represent the location of city-managed ash trees, as geolocated from their street addresses (Street Tree General Data, 2010). The latter explains why city-managed trees appear to be located within private lots. In our baseline specification, we aggregate tree cover at the postal code level, which mitigates the repercussions of such approximation.

1.3 EAB infestation and the tree canopy

We now discuss important evidence on the effect of the EAB infestation on the evolution of urban forestry between 2007 and 2018. We first provide an illustration of the systematic removal of infested ash trees by focusing on the North-East of Toronto where we observe a relatively high density of publicly maintained ash trees at baseline. Figure 2 compares the land classifications provided by Urban Forestry in 2007 and in 2018 around James Park Square, in the municipal area of Scarborough. There is a marked decrease in the area covered by trees which coincides with the location of city-managed ash trees (green symbols). We provide an additional illustration of such tree felling in Appendix A.2 with successive street views of the same neighborhood in 2007 (before the infestation), 2014 (after the cut-downs), and 2020 (with replanted tree saplings). In the same Appendix A.2, we exploit a register of planned work from Parks and Forestry to discuss the timing and selection of planned removals and TreeAzin injections.

We investigate the systematic relationship between the evolution of urban forestry and tree removals in Figure 3. We consider a postcode as the main unit of observation, and we first construct the long difference in area share of tree cover between 2007 and 2018. Panel (a) of Figure 3 shows the correlation between the evolution of the tree canopy and a measure of ash tree density—the number of street ash trees

Figure 3. The effect of ash tree density on the tree canopy between 2007 and 2018.

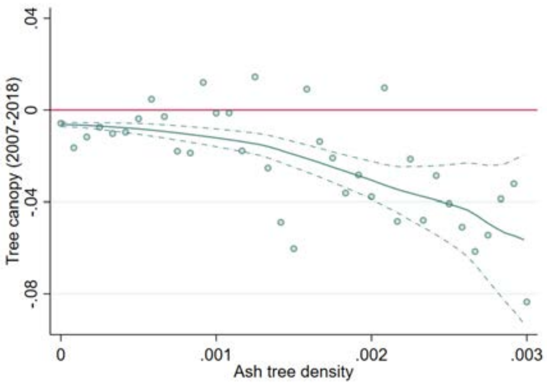

(a) Tree canopy (difference, 2007–2018)

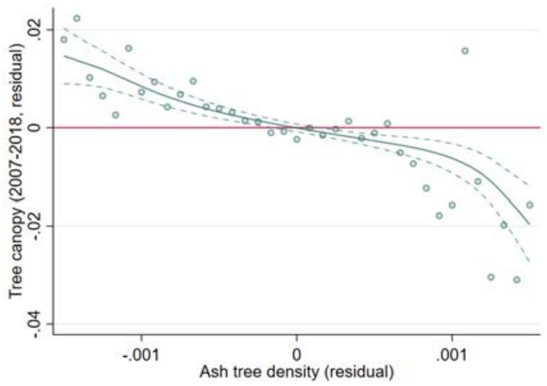

(b) Tree canopy (residual, 2007–2018)

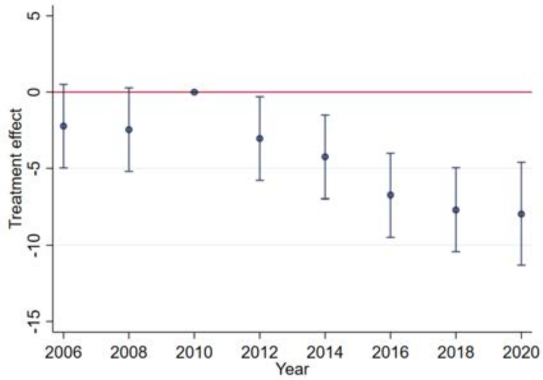

(c) NDVI (2006–2020)

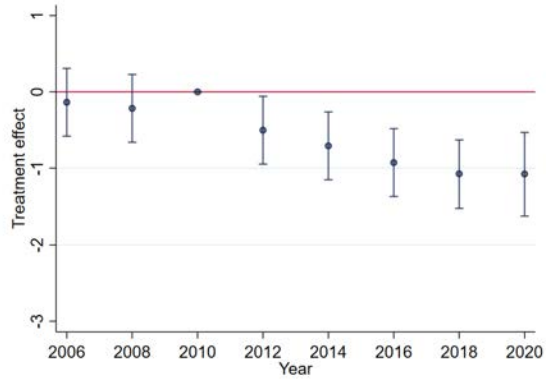

(d) LAI (2006–2020)

Notes: Panel (a) represents the relationship between the evolution of the area share of tree cover between 2007 and 2018 and the density of ash trees within a postal code (number of street ash trees per area within a 10m buffer, as measured in 2010). We group postal codes by bins of ash tree density: the dots represent the average evolution of the tree canopy within each bin. Panel (b) represents the same relationship in which the evolution of the area share of tree cover between 2007 and 2018 and the ash tree density are residualized: we regress both measures on a measure of street tree density, latitude, longitude, area shares from the land classification in 2007 (tree canopy, grass/shrub, bare earth, water, buildings, roads, other paved surfaces and agriculture) and ward fixed effects. The lines are locally weighted regression on all observations. Panels (c) and (d) show the estimated correlation between ash tree density and vegetation cover from 2006 to 2020. More specifically, we regress the Normalized Difference Vegetation Index (NDVI, panel c) and the Leaf Area Index (LAI, panel d) across postcodes on: a measure of ash tree density (number of street ash trees per area within a 10m buffer, as measured in 2010); a measure of street tree density; ward fixed effects; latitude, longitude; dummies for the land classification in 2007 (tree canopy, grass/shrub, bare earth, water, buildings, roads, other paved surfaces and agriculture)—all interacted with year fixed effects. The reported coefficients are the ones in front of the measure of ash tree density interacted with period fixed-effects, and vertical lines show 95 percent confidence intervals. Both indices are obtained by combining the reflection in the near-infrared spectrum (NIR) with the reflection in the visible range of the spectrum and rely on a cloud-free mosaic of Landsat imagery (L7/L8, 30m resolution) covering May–September from 2006 to 2020.

per area , as measured in 2010—across postcodes. Panel (b) conditions this relationship on a measure of street tree density (irrespective of their species), latitude, longitude, the land classification in 2007 (the area shares of tree canopy, grass/shrub, bare earth, water, buildings, roads, other paved surfaces and agriculture) and ward fixed effects. We find that there is a strong, precisely estimated, negative correlation between the evolution of tree cover from 2007–2018 and the initial density of ash trees: an additional 0.003 ash trees per square meter is associated with a decrease of 0.04 in the area share of tree cover (see panel b for instance). To rationalize the previous relationship, an additional 0.003 ash tree per square meter corresponds to 3,000 ash trees per square kilometer. If each ash tree uniquely covered about 35 square meters, these 3,000 ash trees would cover 10% of a square kilometer.[13] Compared to this back-of-the-envelope calculation, the actual tree cover decreases by only 4-5% of a square kilometer. The difference between the two numbers could be explained by: (i) significant overlap between tree crowns; (ii) sluggish tree removals and trees having received TreeAzin injections; and (iii) fast replacement by tree saplings.

The previous evidence quantifies the swift loss of urban forestry in postal codes with numerous ash trees. We shed additional light on the average timing of such loss in panels (c) and (d) of Figure 3. To do so, we leverage yearly vegetation indices constructed from satellite imagery and run an event-study specification estimating the relationship between vegetation indices, I_{pt}, in postcode p at time t (we group years into two-year periods) and our baseline measure of exposure to the EAB infestation, $A_{p,2010}$:

$$I_{pt} = \sum_{\tau=2006}^{\tau=2020} \beta_\tau A_{p,2010} \times \mathbb{1}_\tau + \gamma_t \mathbf{X}_p + \eta_p + \mu_t + \varepsilon_{pt},$$

where $\mathbf{X}_p$ includes: a measure of street tree density; ward fixed effects; latitude, longitude; area shares for each land category in 2007 (tree canopy, grass/shrub, bare earth, water, buildings, roads, other paved surfaces and agriculture)—all interacted with year fixed effects γ_t. Panels (c) and (d) of Figure 3 show that the differential dynamics of vegetation indices across neighborhoods materialize from 2012 onward with most of the vegetation loss occurring before 2016. An additional 0.003 ash trees per square meter leads to an incremental decrease in the Normalized Difference Vegetation Index of $0.003 \times 7 \approx 0.021$ (to be compared with its standard deviation of 0.14 across postal codes) and in the Leaf Area Index of $0.003 \times 1.15 \approx 0.0035$ (to be compared with its standard deviation of 0.02 across postal codes). Both amount to a loss of 15% of a standard deviation, which is a very significant vegetation loss over a period of 4-5 years. Equally important is the observation that there is no

[13] The crown radius of the average (lost) ash tree is not observable in our data. We do, however, observe the diameter at breast height of injected trees (28.7 cm on average) and non-injected trees (29.1 cm on average)—the latter constituting arguably the bulk of our "compliers", i.e., the population of trees lost between 2007–2018. These diameters at breast height would imply an average crown radius of 3.3-3.4m using the relationships estimated in Hemery et al. (2005) for Fraxinus excelsior or Peper et al. (2014) for Fraxinus americana. The equivalent crown radius would be 4m using the (cruder) ratio between crown radius and diameter at breast height of 14 (Lockhart et al., 2005).

immediate rebound in tree cover: the felling of mature trees cannot be mitigated in the shorter and medium run; growing a proper substitute to maturity should take about 25-30 years.

Table 1. Ash trees and the evolution of the tree canopy between 2007 and 2018.

Tree cover (2007–2018)	(1)	(2)	(3)
Ash tree density	-12.23	-13.78	-13.96
	(1.349)	(1.365)	(1.372)
Street tree density		1.444	1.910
		(0.197)	(0.287)
Spruce tree density			1.189
			(1.305)
Elm tree density			3.408
			(2.042)
Maple tree density			-2.000
			(0.575)
Observations	45,520	45,520	45,520

Notes: Robust standard errors are reported between parentheses. The unit of observation is a postcode in the City of Toronto, and the dependent variable is change in the area share of tree cover between 2007 and 2018. All specifications include: ward fixed effects; latitude and longitude; and area shares from the land classification in 2007 (tree canopy, grass/shrub, bare earth, water, buildings, roads, other paved surfaces and agriculture). In column (2), we add the number of public trees normalized by the postcode area. In column (3), we add the number of spruce trees, elm trees and maple trees normalized by the postcode area.

Finally, our identification exploits the unanticipated, random occurrence of an ecological catastrophe to isolate exogenous variation in urban forestry. However, our instrumental variable is based on the initial location of vulnerable, *city-managed* trees. The correlation between the initial distribution of a specific tree species and the dynamics of tree cover could theoretically be driven by other urban policies, e.g., aimed at diversifying the green capital within the city. We explore the relationship between the evolution of the tree canopy from 2007–2018 and the density of publicly maintained trees in Table 1. In this table, as in Figure 3, the unit of observation is a postal code, the dependent variable is the change in tree cover between 2007 and 2018, and we control for ward fixed effects, latitude and longitude, and area shares of trees, grass/shrub, bare earth, water, buildings, roads, other paved surfaces and agriculture in 2007. In column (2), we add a control for the density of all publicly maintained trees within a 10m buffer of the postcode. In column (3), we add the densities of other popular species of publicly maintained trees (i.e., spruce trees, elm trees, maples). The negative effect of the initial density of ash trees is robust across specifications and is one order of magnitude larger than the effects of other tree species. This ash-specific effect is key to supporting our empirical strategy: the initial distribution of city-managed trees should only capture the quasi-random allocation of an otherwise common tree species across space and be orthogonal to concurrent planning policies or green initiatives.

2 Empirical strategy

This section describes the empirical strategy and a few descriptive statistics.

2.1 Estimating the hedonic value of the tree canopy

The hedonic value of urban forestry should encompass all the net present benefits of a tree in a given proximity to a property, including its long-term effect on energy consumption. An empirical strategy aiming to estimate the causal effect of trees on property values should exploit exogenous and permanent shocks to the tree canopy. The shock used in this paper is the initial relative allocation of city-managed ash trees that will (mostly) be lost to the Emerald Ash Borer infestation and thus affect tree cover in the medium and longer run—as documented in the previous section.

A naive empirical strategy would correlate transaction prices with local tree cover, possibly controlling for time-invariant local characteristics and trends along some observables. Such a specification would suffer from three major issues: omitted variation, reverse causality, and measurement error. First, the dynamics of urban forestry may relate to local developments, for instance, neighborhood quality, investments in green infrastructure, transport infrastructure, or the construction of new offices. Each of these sources of omitted variation would strongly affect property prices and lead to changes in the tree canopy. Second, a rise in the local price of land increases the opportunity cost of maintaining urban forestry. Third, the measure of tree density may be contaminated by measurement error related to the procedures employed to evaluate the tree canopy.

We address these identification issues by isolating variation in the tree canopy generated by an irreversible and exogenous shock: the Emerald Ash Borer infestation. Letting i denote a transaction with associated price P_{ipt} and TD_{pt} denote the inferred area share of tree canopy within the postcode p at time t, we estimate:

$$\ln(P_{ipt}) = \alpha + \beta TD_{pt} + \gamma_{\mathrm{t}} \mathbf{X}_{ipt} + \eta_p + \mu_t + \varepsilon_{ipt}, \tag{1}$$

where TD_{pt} is instrumented by the density of publicly managed ash trees, A_{pt}, and

$\gamma_t \mathbf{X}_{ipt}$ captures the evolution of the time-varying premium associated to: observable house characteristics (i.e., number of bedrooms and number of washrooms); ward fixed effects; a measure of city-managed tree density; latitude and longitude; and area shares from the land classification in 2007 (tree canopy, grass/shrub, bare earth, water, buildings, roads, other paved surfaces and agriculture). The specification thus flexibly controls for the differential evolution of prices across neighborhoods and time-varying returns to house characteristics. Standard errors are clustered at the postcode × year level in the baseline specification, but we consider alternative clustering strategies in robustness checks.

Equation (1) requires measures that capture the evolution of tree density, TD_{pt}, and ash tree density, A_{pt}. We do not have detailed information on the yearly evolution of the tree canopy: we only observe it at the time of the surveys conducted in 2007 and 2018. We do however know from records of the City of Toronto that 2011 is the beginning of work orders to remove ash trees that were infested with the Emerald Ash Borer, with a marked acceleration in 2013—an observation that is confirmed by our less precise measures of land cover at the yearly level sourced from satellite imagery (see Figure 3).[14] We thus construct the baseline exposure to urban forestry and the baseline instrument as follows: $TD_{pt} = TD_{p,2007}$ for $t \leq 2013$ and $TD_{pt} = TD_{p,2018}$ for $t \geq 2016$, $A_{pt} = A_{p,2010}$ for $t \leq 2013$ and $A_{pt} = 0$ for $t \geq 2016$, and we interpolate linearly both measures TD_{pt} and A_{pt} between 2013 and 2016.

With forward-looking agents capitalizing the future flow of amenities provided by urban forestry, property prices should reflect future tree removals once the information about the EAB infestation becomes public. One assumption behind our strategy is that the vast majority of anticipated tree removals occur before 2018 such that all lost publicly-managed ash trees are already captured within our measure of urban forestry in 2018. Imperfect "compliance" from a few remaining trees that would be expected to disappear after 2018 would lead to an over-estimate of the hedonic value of urban forestry. Further, we cannot really observe the evolution of the information set of land market participants. For this reason, we provide robustness checks with alternative cut-offs and without any inference to show that the previous inference is not driving our main findings. For instance, we can focus on a sub-sample of property transactions covering (i) a *pre-treatment period* between 2007–2009, where no EAB-related damages had occurred yet; and (ii) a *post-treatment period* between 2016–2017 when the majority of ash trees had been removed.

The identification of specification (1) hinges on the assumption that the alloca-

[14] We observe one work order for an ash tree removal in 2010; 1,646 work orders for ash tree removals in 2011; 3,912 in 2012 and 7,151 in 2013. Unfortunately, we do not have data for later years.

Table 2. Descriptive statistics.

	Mean	Stand. dev.	Tree density High	Tree density Low
Panel A: Transaction characteristics				
Transaction price	13.03	0.627	13.20	12.86
Number of bedrooms	1.981	1.351	2.331	1.630
Number of washrooms	2.182	1.114	2.479	1.886
Panel B: Land cover in 2007				
Tree canopy	0.220	0.191	0.380	0.060
Grass/shrub	0.152	0.121	0.181	0.123
Bare earth	0.009	0.083	0.001	0.017
Water	0.001	0.007	0.001	0.001
Buildings	0.225	0.161	0.192	0.259
Roads	0.161	0.165	0.114	0.207
Other paved surfaces	0.229	0.218	0.129	0.330
Agriculture	0.000	0.003	0.000	0.000
Panel C: City-managed trees				
Ash trees (density, per sq. km)	78.28	263.2	89.59	66.98
All trees (density, per sq. km)	1,949	2,083	2,164	1,734
Observations	385,933		192,839	193,094

Notes: All statistics are computed using the baseline sample of transactions. The samples of high- and low-tree density are defined with respect to the median share of tree canopy as produced by Urban Forestry as part of an Urban Tree Canopy Assessment in 2007.

tion of ash trees is orthogonal to the evolution of residential prices at the postcode level—conditioning on the evolution of the overall number of public trees. This empirical strategy may be threatened by the possible correlation between the spatial distribution of ash trees, inherited from the earlier spatial distribution of elm trees, and neighborhood dynamics in the City of Toronto. For instance, neighborhoods may go through long cycles related to the age of the housing stock (Brueckner and Rosenthal, 2009), and growing areas in the 1930s may now experience a gentrification from the redevelopment of historic neighborhoods. We provide reassuring evidence about this threat by assessing the existence of pre-treatment differential trends between 2002 and 2006.

2.2 Descriptive statistics

Before we move on to the main estimation, this subsection provides some descriptive statistics that aim to provide a better understanding of the variation underlying the identification strategy.

We start by reporting descriptive statistics about transaction data in Table 2: the mean and standard deviations of the main variables, control variables and their values for transactions in postal codes with above- or below-median tree canopy. As apparent in Table 2, there are wide differences in tree density across properties. Postcodes with above-median tree density have almost six times more tree cover than postcodes with below-median tree density in 2007. Urban forestry correlates with property prices, which are about 40% higher for properties with above-median tree density. This price differential may illustrate a tree premium, but they also seem to indicate differential property characteristics: Properties with above-median tree density have, on average, 0.6 additional bedrooms and one additional washroom.

Figure 4. Housing prices, temperature, and density of the tree canopy.

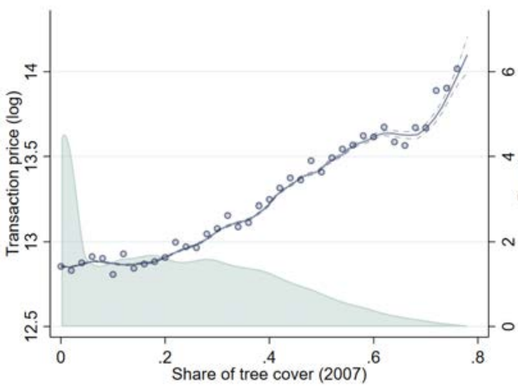

(a) Housing prices

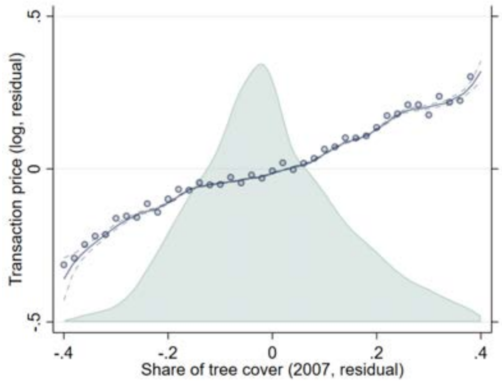

(b) Housing prices (res.)

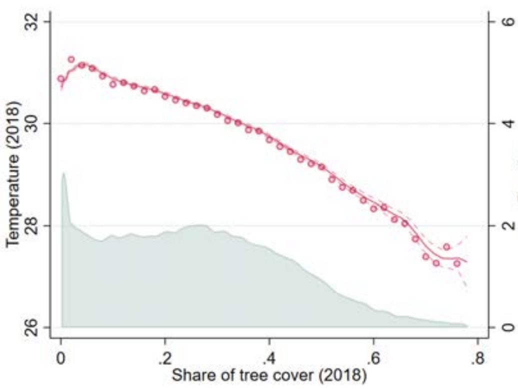

(c) Temperature

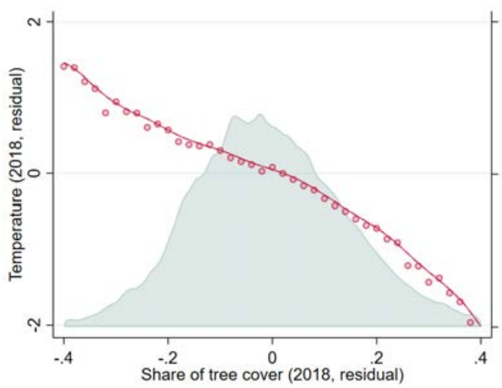

(d) Temperature (res.)

Notes: Panel (a) represents the relationship between the (logarithm) transaction price and our measure of tree cover at the postcode level. We group transactions by bins of tree cover: the dots represent the average transaction price within each bin. The green area represents the distribution of the x-axis variable across all panels. Panel (b) represents the same relationship in which the (logarithm) transaction price and the tree cover within the postcode are residualized: we regress both measures on the number of bedrooms, the number of washrooms, the latitude, the longitude, ward fixed effects—all interacted with year fixed effects. Panel (c) represents the relationship between the average temperature during the summer in 2018 and our measure of tree cover at the postcode level (with a buffer of 10m around the postcode shape and in 2018). We group postcodes by bins of tree cover: the dots represent the average temperature within each bin. Panel (d) represents the same relationship in which the temperature and the tree cover within the postcode are residualized: we regress both measures on the latitude, the longitude, and ward fixed effects. The lines are locally weighted regression on all observations.

Panels (a) and (b) of Figure 4 show the correlation between house prices and the surrounding urban forestry. The x-axis is the area share of tree cover in 2007, TD_{p2007}; and the y-axis is the average (log) house price. The association between transaction prices and tree density should reflect the price premium associated with leafy suburbs, but also the opportunity cost of maintaining urban forestry. As shown in panel (a), this correlation is positive for almost any share of tree cover in 2007, especially so in residential areas with significant urban forestry. Panel (b) displays the same relationship conditioning on our main control variables: the number of bedrooms and washrooms; latitude, longitude; and ward fixed effects—all interacted with year fixed effects. As apparent, the price gradient between less and more leafy neighborhoods remains substantial. Panels (c) and (d) show a strongly negative correlation between summer temperatures (June-September 2018), T_p, and the surrounding urban forestry. There is an average difference of about four degrees Celsius between postcodes with very low versus very high tree cover. This holds true even when conditioning on ward fixed effects and our baseline controls.

3 The hedonic value of urban trees

In this section, we estimate the hedonic value of urban forestry. Our headline finding is that the tree premium is both economically and statistically significant: adding one tree within a postcode increases property prices by 0.40%.

3.1 Baseline specification

Table 3 reports the estimates of Equation (1). By default, all estimations are conditioned on postcode fixed-effects and year fixed effects interacted with: eight categories of land cover in 2007; the density of city-managed trees; latitude; longitude; and ward-fixed effects. Column (1) reports OLS estimates; and columns (2) and (3) report IV estimates in which the evolution in tree density between 2007 and 2018, TD_{pt}, is instrumented by the density of ash trees, A_{pt}. In column (3), we add transaction controls, i.e., the number of bedrooms and washrooms interacted with year fixed effects to control for valuations of house characteristics that are allowed to vary over time in a flexible manner.

The OLS specification shows that the correlation between tree density and property values is negative and quantitatively irrelevant (column 1). The IV specification finds instead a positive and significant causal effect of urban forestry on property prices. One additional percentage point in tree cover within a postcode increases property values by 0.86% in our preferred specification (column 3). To help under-

Table 3. The amenity value of trees—baseline specification.

Transaction price (log)	(1)	(2)	(3)
Tree cover	-0.049	1.009	0.866
	(0.015)	(0.310)	(0.272)
Transaction controls	No	No	Yes
Observations	374,295	374,295	374,286
F-statistic	-	80.73	83.82

Notes: Standard errors are reported between parentheses and are clustered at the postcode × year level. Column (1) reports OLS results and columns (2)-(3) report the estimates from the IV specification in which tree cover is instrumented by the the density of city-managed ash trees. The unit of observation is a transaction, and the dependent variable is the (log) transaction price. All specifications are weighted by the inverse of the number of observations in a given postcode. All specifications include: (i) postcode fixed effects; (ii) ward fixed effects interacted with year fixed effects; (iii) a measure of city-managed tree density interacted with year fixed effects; (iv) latitude and longitude interacted with year fixed effects; and (v) area shares from the land classification in 2007 (tree canopy, grass/shrub, bare earth, water, buildings, roads, other paved surfaces and agriculture) interacted with year fixed effects. The set of transaction controls include the number of washrooms and bedrooms interacted with year fixed effects.

stand the magnitude of these estimates, consider the following thought experiment: the average non-injected ash tree increases the tree canopy by about 35 square meters; the average postcode covers about 8,000 square meters; thus, one additional tree increases the area share of tree canopy by 0.45 percentage points. Using our preferred estimate, this additional tree would cause a property price increase of about 0.40%. Alternatively, postal codes that were most affected by the ecological catastrophe had an initial density of (city-managed) ash trees around 0.005; the loss in the area share of tree cover would amount to $0.005 \times 13.78 \approx 0.07$ (column 2 of Table 1) leading to a drop in housing prices around $0.07 \times 0.866 \approx 6\%$.

This average treatment effect masks significant heterogeneity. We shed some light onto the heterogeneity of treatment effects across more or less deprived postal codes, postal codes with more or less urban trees at baseline, and across property characteristics (single-unit versus multi-unit buildings) in Appendix B. We find that the tree premium is larger in more affluent neighborhoods. More strikingly, we find that a marginal tree is only valued in neighborhoods with significant tree cover, in line with the shape of the price gradient in urban forestry depicted in Panel (a) of Figure 4. Demand for urban forests thus depends on many factors (see, for instance, Zhu and Zhang, 2008), and one important driver is the pre-existing state of local green infrastructure.

3.2 Identification and robustness checks

One threat to identification is that the initial distribution of ash trees, partly reflecting urban developments in 1900–1930 and the associated distribution of elm trees, correlates with secular neighborhood dynamics. We reduce concerns about this identification threat by testing for the existence of pre-treatment differential trends. Specifically, we consider the period 2002–2006 in which we do observe property transactions, albeit with limited transaction controls, and estimate Equation (1) on this sample of transactions displacing treatment and the transition of land cover between 2007–2018 from 2013–2016 to 2004–2005. It is reassuring that Panel A of Table 4 shows no differential trends before the treatment date: the OLS estimate (column 1) is similar to that obtained on the baseline sample, but the IV estimate (column 2) is small, negative, and non-significant.

We then provide a systematic sensitivity analysis around the baseline specification in the remainder of Table 4. In Panel B, we construct the baseline exposure to urban forestry and the baseline instrument as follows: $TD_{pt} = TD_{p,2007}$ for $t \leq T_1$ and $TD_{pt} = TD_{p,2018}$ for $t \geq T_2$, $A_{pt} = A_{p,2010}$ for $t \leq T_1$ and $A_{pt} = 0$ for $t \geq T_2$. However, we do not interpolate between T_1 and T_2 and rather exclude the years in between. In short, this specification is equivalent to defining a pre-treatment period $[2007, T_1]$ and a post-treatment period $[T_2, 2017]$. Panel B shows that our main estimate varies between 0.70 and 0.90, when the pre-treatment period changes from $[2007, 2011]$ to $[2007, 2009]$ and the post-treatment period from $[2014, 2017]$ to $[2016, 2017]$. In Panel C, we consider a long difference setting, similar in essence to the previous exercise, but rather collapse the data at the postcode level. The estimated equation is:

$$\Delta \ln(P_p) = \alpha + \beta \Delta TD_p + \gamma \mathbf{X}_p + \varepsilon_p \tag{2}$$

where ΔTD_p is instrumented by $A_{p,2010}$, and controls (e.g., transaction characteristics, land cover in 2007) are collapsed at the postcode level. The estimate varies between 0.70 and 1 when we change the pre-treatment period from $[2007, 2011]$ to $[2007, 2009]$ (and the post-treatment period from $[2014, 2017]$ to $[2016, 2017]$). In Panel D, we consider minor alterations around our baseline specification: we construct land cover and ash tree density with a 20m buffer in column (1), instead of 10m; we winsorize non-zero values for ash tree density and all street tree density at 90% or 99%, rather than at 95% in the baseline. Again, the exercise confirms the robustness of our baseline estimations. In Panel E, we condition on time-varying dependence in amenities (distance to green areas, ravines, schools, area share of sidewalk, length of pedestrian paths), in topography (elevation, slope), and in neighborhood income at baseline. Lastly, in Panel F, we consider alternative clustering procedures: at the postcode level in column (1); at the ward × year level in column (2); and at the ward level in column (3). Even in the most demanding specification with about 50 clusters at the level of wards, our estimated effects remain significantly different from 0 at the 10%-level.

4 The cooling effect of urban forestry

The previous section has shown that there is an amenity value to local urban forestry. One possible component of this value derives from the cooling effect of the tree canopy during heat waves. We explore this specific effect in two steps. First, we look at local temperatures during summer and subsequently, we analyze energy consumption.

Urban forestry and urban heat Urban forestry arguably reduces the urban heat island effect (Oke, 1973; Roy et al., 2012). Our experiment provides a natural setting to quantify such an effect, as we isolate exogenous variation in the evolution of the tree canopy within postcodes over time. This design alleviates concerns that households residing in green neighborhoods are inherently more environmentally conscious and, consequently, utilize energy more judiciously, but also addresses the alternate concern that wealthier households gravitate toward greener neighborhoods, which could potentially result in higher energy consumption.

To investigate this relationship, we consider the following specification,

$$T_{pt} = \alpha + \beta TD_{pt} + \gamma_t \mathbf{X}_p + \eta_p + \mu_t + \varepsilon_{pt}, \tag{3}$$

where each observation is a postal code in a given year (see Panel A of Table 5), T_{pt} is the average Land Surface Temperature within postcode p during July and August of that year, and urban forestry, TD_{pt}, is instrumented by the density of ash trees, A_{pt}. Controls include postcode fixed effects and: latitude and longitude; the density of publicly maintained trees; and area shares from the land classification in 2007, all interacted with year fixed effects. As shown in Table 5, urban forestry significantly reduces urban heat during summer months: one additional percentage point in tree cover within a postcode reduces temperature by about 0.05 degrees (Celsius). The most affected postal codes have lost an area share of 0.07 in tree cover to the Emerald Ash Borer infestation; as a result, the average temperature during July and August is now 0.35 degrees (Celsius) higher.

We shed additional light on the gradual effect of the ecological catastrophe in postal codes with high density of city-managed ash trees in Appendix C.1, where we see an increasingly negative effect from 2010 to 2018. This increase reflects higher treatment compliance over time, i.e., ash trees are cut down in a gradual manner as illustrated in Section 1.3, but also secular trends in summer temperatures due to climate change. Global warming is indeed expected to increase temperatures across neighborhoods in Toronto; the previous exercise sheds some light on the value of trees in reducing urban heat island effects in the future.[15]

Urban forestry and energy savings Urban forestry reduces temperatures during the warm summer months, which should affect energy consumption, e.g., through less frequent recourse to air conditioning.

We investigate this energy saving effect in Panel B of Table 5 where we replicate the exercise performed in Panel A of Table 5 with the electricity consumption during July and August as the main dependent variable. One shortcoming is that we do not observe consumption at the beginning of the treatment period, but for intermediate and post-catastrophe years (2012–2020). We thus consider a stacked specification, similar to that of Equation (3), but without postcode fixed-effects. Table 5 shows that one additional percentage point in tree cover within a postcode reduces the average consumption during the summer months by about 2.5% which corresponds to CAD 5 per month.

Appendix C considers two alternative specifications. First, Appendix C.1 documents the gradual energy-consumption effect of the Emerald Ash Borer infestation in postal codes with high density of city-managed ash trees and provides a placebo experiment based on winter months. Second, we consider an alternative specification exploiting short-term weather fluctuations interacted with solar exposure induced by the positioning of trees and solar angles in Appendix C.3. Such an approach also allows us to better characterize the (limited) sheltering effect of urban forestry during winter months: trees play a role in reducing heat effects in the summer, but can also provide some shelter from wind in the winter.

The quantitative role of energy savings How do these energy savings compare with the hedonic value of urban trees? When smoothed over a period of 12 months, one additional percentage point in tree cover reduces energy consumption by 0.4% through its cooling effect, and by 0.1% through its wind-sheltering properties (see Appendix C.4). Those cumulative effects would amount to CAD 1 per month. In

[15] Appendix A.4 provides additional visual illustrations of the relationship between local summer temperatures and the local extent of the tree canopy—focusing on a heat wave in 2018. We study non-linearities in the cooling and energy-saving effects of trees in Appendix B.2.

comparison, the associated increase in the flow value of a property of 0.86% would correspond to CAD 21 per month—a calculation based on the fact that the average monthly rent for a two-bedroom apartment was around CAD 2,500 in 2018.

Could the expected rise in global temperatures and the exacerbation of urban heat island effects account for the disparity between the estimated energy-saving premium and the discounted hedonic value of urban trees? The latter, after all, is intended to encompass all future discounted benefits of urban trees. Our back-of-the-envelope calculations do not support such an interpretation. While global warming is projected to increase the energy-saving premium, this is not enough to explain the full extent of the hedonic value attributed to urban trees. The number of annual hours with average temperatures surpassing 30 degrees Celsius is expected to double between 2020 and 2050, transitioning from the equivalent of 10 to 20 days. Moreover, there exists a non-linear relationship between temperature and energy consumption during the summer months (see Appendix C.4). Even under an extreme scenario, global warming would at most explain a doubling of the energy-saving premium by 2050. While this increase would be substantial, it remains one order of magnitude too small to explain the hedonic value of urban trees.

The energy benefits derived from urban forests alone outweigh the maintenance costs of urban forestry. The addition of a single tree within a postcode results in a 0.45 percentage point increase in the area covered by the tree canopy and leads to an annual energy consumption reduction of approximately CAD $12 \times 1 \times 0.45 \approx 5.40$ *per household*. Given that there are roughly 20 households per postcode, the total energy-saving benefit derived from a tree exceeds CAD 100. This is an order of magnitude greater than the annual maintenance cost, which was estimated at approximately CAD 4.20 according to the 2011 City of Toronto Parks and Forestry budget proposal. While these calculations do not account for the opportunity cost of land, including this factor would not alter the conclusion of a net benefit attributable to urban trees, considering that the energy-saving effect of urban forestry pales in comparison to its amenity value.

5 Concluding remarks

This paper assesses the value of urban trees. This is a challenging empirical exercise because of (i) omitted variation affecting tree density and demand for neighborhoods (e.g., neighborhood quality) and (ii) reverse causation (e.g., land prices affecting the opportunity cost of maintaining urban forestry). To establish causality and present robust quantitative estimates, we exploit large, persistent and quasi-experimental variation stemming from the Emerald Ash Borer infestation in Toronto. We find that the hedonic value of urban forestry far outweighs the associated maintenance costs, rendering it a highly profitable investment.

Existing research has shown that trees have a number of beneficial effects on their environment which may contribute to this estimated amenity effect. For instance, Nowak and Aevermann (2019) provide a valuation toolbox accounting for the discounting of future benefits and possible replacement; Kardan et al. (2015) highlight the positive effect of trees on mental health in a study that uses the 2007 canopy survey in Toronto; and a recent study by Jones and McDermott (2018b) analyzes how the loss of ash trees leads to increased air pollution across American cities.[16] Less research has systematically explored the energy-saving potential offered by the urban tree canopy. Leveraging novel data on energy consumption, our study reveals that trees effectively lower local temperatures during heatwaves, resulting in substantial energy savings. While this energy-saving aspect is significant and expected to gain even greater importance in the future, particularly as temperatures and energy costs continue to rise, it is noteworthy that these direct monetary benefits fall short of accounting for the full amenity value associated with urban forestry. One plausible explanation for this discrepancy is that the substantial cooling effect provided by urban forestry is not solely confined to energy consumption; it also has a direct positive impact on the well-being of residents by creating cooler living environments both indoors and outdoors. Additionally, previous research has established that trees offer a variety of amenity effects, which are all capitalized in house prices. Through an indirect analysis, we discover that these other facets explain a significant portion of the "tree premium."

While the qualitative understanding that urban forestry confers benefits to urban residents is not surprising, our *quantitative* findings offer additional insights that are both novel and striking. We demonstrate that substantial private benefits are already accrued from the cooling attributes of urban forestry, and the predicted change in temperature over the coming decades will further exacerbate demand for green infrastructure to provide shade and evapotranspiration. Moreover, urban residents place a high value on urban forests that extends well beyond the realm of energy savings. This strong and apparent demand for urban forestry stands in stark contrast to the observed public policies in place. In numerous North American cities, there is a relatively modest, and in percentage terms, even *decreasing* inventory of urban trees, as documented in prior studies (e.g., Nowak and Greenfield, 2012, 2018). Several

[16] We find a similar (moderate) effect for the concentration of small particles across neighborhoods of Toronto during summer, as shown in Panel C of Table 5. We provide a detailed description of the data in Appendix D, together with a discussion about the dynamics of such a pollution-abatement effect and a placebo exercise focusing on the effect of trees during winter.

explanations might account for this misalignment. It is possible that governments have yet to fully internalize the costs associated with climate change or may fail to fully recognize the perceived value of urban forestry. Alternatively, coordination issues could be at play. We uncover that the valuation of urban forestry is nonlinear, with the marginal effect only manifesting in areas with a substantial existing tree cover. Given that cities or neighborhoods with limited green infrastructure often correspond to economically disadvantaged areas, policy interventions targeting such cities or regions could potentially address not only coordination challenges but also generate significant redistributive effects.

Table 4. The amenity value of trees—robustness checks.

Transaction price (log)	(1)	(2)	(3)
Panel A: Placebo specification (2002-2006)			
Tree cover	-0.067	-0.197	
	(0.020)	(0.388)	
Observations	168,457	168,457	
F-statistic	-	48.26	
Panel B: No inference			
Tree cover	0.707	0.874	0.901
	(0.198)	(0.454)	(0.315)
Sample	S1	S2	S3
Observations	311,261	240,448	168,598
F-statistic	115.44	79.72	51.66
Panel C: Long difference			
Tree cover	0.761	1.006	0.934
	(0.333)	(0.385)	(0.310)
Sample	S1	S2	S3
Observations	21,264	18,404	14,312
F-statistic	64.93	55.48	41.26
Panel D: Sensitivity			
Tree cover	1.378	1.013	0.795
	(0.418)	(0.314)	(0.298)
Exposure	Buffer: 20m	Winsorizing: 90%	Winsorizing: 99%
Observations	370,556	374,286	374,286
F-statistic	30.33	65.12	48.07
Panel E: Additional controls			
Tree cover	0.803	0.881	0.858
	(0.265)	(0.264)	(0.275)
Controls	Amenities	Topography	Income
Observations	374,286	364,737	374,286
F-statistic	86.79	90.74	81.84
Panel F: Clustering			
Tree cover	0.866	0.866	0.866
	(0.345)	(0.290)	(0.485)
Clustering	Postcode	Ward × year	Ward
Observations	374,286	374,286	374,286
F-statistic	40.41	38.57	9.86

Notes: Standard errors are reported between parentheses and are clustered at the postcode × year level (except in Panel F). All columns report the estimates from the IV specification in which tree cover is instrumented by the ash tree density. In Panel B, D, E and F, the unit of observation is a transaction, the dependent variable is the (log) transaction price, and the specifications include: (i) postcode fixed-effects; (ii) ward fixed effects interacted with year fixed effects; (iii) a measure of street tree density interacted with year fixed effects; (iv) latitude and longitude interacted with year fixed effects; (v) area shares from the land classification in 2007 (tree canopy, grass/shrub, bare earth, water, buildings, roads, other paved surfaces and agriculture) interacted with year fixed effects; and (vi) the number of washrooms and bedrooms interacted with year fixed effects (except in Panel A, mirroring Table 3). All specifications are weighted by the inverse of the number of observations in a given postcode. In Panel A, the sample consists of observations between 2002 and 2006 (excluded from our baseline sample), and the dependent variable is constructed using a treatment date in 2004. In Panel B, we restrict the sample to 2007–2011/2014–2017 in column (1), 2007–2010/2015–2017 in column (2), 2007–2009/2016–2017 in column (3). In Panel C, we apply the same sample restrictions and consider a specification in long difference in which all variables are collapsed at the postcode level. In Panel D, we explore variations around the baseline specification: a buffer of 20m around postcodes in column (1), a winsorizing at 90% for public and ash tree densities in column (2), a winsorizing at 99% for public and ash tree densities in column (3). In Panel E, we condition on time-varying dependence in: amenities (distance to green areas, ravines, schools, area share of sidewalk, length of pedestrian paths), topography (elevation, slope), and neighborhood income at baseline. In Panel F, we explore variations around the baseline clustering procedure: at the postcode level in column (1), at the ward × year level in column (2), at the ward level in column (3). There are about 50 wards in Toronto.

Table 5. The cooling effect of trees—temperature, energy consumption, and pollution.

Land Surface Temperature (LST)	(1)	(2)
Panel A: Temperature		
Tree cover	0.195	-5.144
	(0.049)	(1.059)
Observations	702,138	702,138
F-statistic	-	646.49
Electricity usage	**(1)**	**(2)**
Panel B: Electricity consumption		
Tree cover	0.077	-2.483
	(0.015)	(0.516)
Observations	280,931	280,931
F-statistic	-	217.64
Pollution (PM2.5)	**(1)**	**(2)**
Panel C: PM2.5 concentration		
Tree cover	-0.005	-0.120
	(0.001)	(0.015)
Observations	373,610	373,610
F-statistic	-	548.50

Notes: Robust standard errors are reported between parentheses. The unit of observation is a postcode. Across both panels, column (1) reports the OLS estimate while column (2) reports the estimates from an IV specification where tree cover is instrumented by a measure of ash tree density. All specifications include: latitude and longitude; the density of publicly maintained trees; and area shares from the land classification in 2007, all interacted with year fixed effects. In Panel A, the dependent variable is the Land Surface Temperature (LST) computed as an average during July/August, and we control for postcode fixed effects. In Panel B, the dependent variable is the (log) electricity consumption in July/August for the median household within a postal code and for all years between 2012–2020, and we control for ward fixed effects. In Panel C, the dependent variable is (log) concentration of PM2.5 in July/August (in $\mu g/m^3$), and we control for postcode fixed effects (see Appendix D).

References

Akbari, H. and H. Taha, "The impact of trees and white surfaces on residential heating and cooling energy use in four Canadian cities," *Energy*, 1992, *17* (2), 141–149.

Auffhammer, Maximilian, "Climate Adaptive Response Estimation: Short And Long Run Impacts Of Climate Change On Residential Electricity and Natural Gas Consumption Using Big Data," NBER Working Papers 24397, National Bureau of Economic Research, Inc 2018.

Aukema, Juliann E., Brian Leung, Kent Kovacs, Corey Chivers, Kerry O. Britton, Jeffrey Englin, Susan J. Frankel, Robert G. Haight, Thomas P. Holmes, Andrew M. Liebhold, Deborah G. McCullough, and Betsy Von Holle, "Economic impact of non-native forest pests in the continental United States," *PLoS One*, 2011, *6* (9).

Barham, L., G. Duller, and et al. Nkombwe P., "Evidence for the earliest structural use of wood at least 476,000 years ago," *Nature*, 2023, *622*, 107–111.

Benson, Earl D, Julia L Hansen, Arthur L Schwartz, and Greg T Smersh, "Pricing residential amenities: the value of a view," *The Journal of Real Estate Finance and Economics*, 1998, *16* (1), 55–73.

Bowler, Diana E., Lisette Buyung-Ali, Teri M. Knight, and Andrew S. Pullin, "Urban greening to cool towns and cities: A systematic review of the empirical evidence," *Landscape and Urban Planning*, 2010, *97* (3), 147–155.

Brueckner, Jan K and Stuart S Rosenthal, "Gentrification and neighborhood housing cycles: will America's future downtowns be rich?," *The Review of Economics and Statistics*, 2009, *91* (4), 725–743.

City of Toronto, "2018 Tree Canopy Study," Technical Report, Report from the General Manager, Parks, Forestry and Recreation 2019.

Conway, Delores, Christina Q Li, Jennifer Wolch, Christopher Kahle, and Michael Jerrett, "A spatial autocorrelation approach for examining the effects of urban greenspace on residential property values," *The Journal of Real Estate Finance and Economics*, 2010, *41* (2), 150–169.

Dell, Melissa, Benjamin F. Jones, and Benjamin A. Olken, "What Do We Learn from the Weather? The New Climate-Economy Literature," *Journal of Economic Literature*, September 2014, *52* (3), 740–98.

Deshmukh, Chandra, Ari Susanto, and et al. Evans Chris, "Evidence for the earliest structural use of wood at least 476,000 years ago," *Nature*, 2023, *616*, 740–746.

Donkelaar, Aaron Van, Melanie S Hammer, Liam Bindle, Michael Brauer, Jeffery R Brook, Michael J Garay, N Christina Hsu, Olga V Kalashnikova, Ralph A Kahn, Colin Lee et al., "Monthly global estimates of fine particulate matter and their uncertainty," *Environmental Science & Technology*, 2021, *55* (22), 15287–15300.

Druckenmiller, Hannah, "Accounting for ecosystem service values in climate policy," *Nature Climate Change*, 2022, *12* (7), 596–598.

_ , "Estimating an Economic Value of Forests: Evidence from Tree Mortality in the American West," Technical Report 2023.

Eichholtz, Piet, Nils Kok, and John M. Quigley, "Doing Well by Doing Good? Green Office Buildings," *American Economic Review*, 2010, *100* (5), 2492–2509.

_ , _ , and _ , "The Economics of Green Building," *The Review of Economics and Statistics*, 2013, *95* (1), 50–63.

Ermida, Sofia L., Patrícia Soares, Vasco Mantas, Frank-M. Göttsche, and Isabel F. Trigoe, "Google Earth Engine open-source code for Land Surface Temperature estimation from the Landsat series.," *Remote Sensing*, 2020, *12*, 1471.

Estrada, Francisco, W. J. Wouter Botzen, and Richard S. J. Tol, "A global economic assessment of city policies to reduce climate change impacts," *Nature Climate Change*, 2017, *7*, 403–406.

Franco, Sofia F and Jacob L Macdonald, "Measurement and valuation of urban greenness: Remote sensing and hedonic applications to Lisbon, Portugal," *Regional Science and Urban Economics*, 2018, *72*, 156–180.

Gatti, Luciana, Camilla Cunha, and et al. Machado Guilherme, "Increased Amazon carbon emissions mainly from decline in law enforcement," *Nature*, 2023, *621.*

Hajat, Shakoor and Tom Kosatky, "Heat-related mortality: a review and exploration of heterogeneity," *Journal of Epidemiology & Community Health*, 2010, *64* (9), 753–760.

Hemery, Gabriel E., Peter S. Savill, and Simon N. Pryor, "Applications of the crown diameter-stem diameter relationship for different species of broadleaved trees," *Forest Ecology and Management*, 2005, *215* (1), 285–294.

Herms, Daniel A. and Deborah G. McCullough, "Emerald ash borer invasion of North America: history, biology, ecology, impacts, and management," *Annual Review of Entomology*, 2014, *59*, 13–30.

Hsu, Angel, Glenn Sheriff, Tirthankar Chakraborty, and Diego Manya, "Disproportionate exposure to urban heat island intensity across major US cities," *Nature communications*, 2021, *12* (1), 2721.

Hubau, Wannes, Simon Lewis, and et al. Zemagho Lise, "A comparative analysis of urban forests for storm-water management," *Nature*, 2020, *579.*

Iungman, Tamara, Marta Cirach, Federica Marando, Evelise Pereira Barboza, Sasha Khomenko, Pierre Masselot, Marcos Quijal-Zamorano, Natalie Mueller, Antonio Gasparrini, JosÃ© Urquiza, Mehdi Heris, Meelan Thondoo, and Mark Nieuwenhuijsen, "Cooling cities through urban green infrastructure: a health impact assessment of European cities," *The Lancet*, 2023, *401* (10376), 577–589.

Jin, Sijia, Jiankang Guo, Stephen Wheeler, Liyan Kan, and Shengquan Che, "Evaluation of impacts of trees on PM2.5 dispersion in urban streets," *Atmospheric Environment*, 2014, *99*, 277–287.

Jones, Benjamin A. and Shana M. McDermott, "The economics of urban afforestation: Insights from an integrated bioeconomic-health model," *Journal of Environmental Economics and Management*, 2018, *89*, 116–135.

_ **and** _ , "Health Impacts of Invasive Species Through an Altered Natural Environment: Assessing Air Pollution Sinks as a Causal Pathway," *Environmental and Resource Economics volume*, 2018, *71*, 23–43.

Kahn, Matthew E. and Randall Walsh, "Cities and the Environment," in Gilles Duranton, J. V. Henderson, and William C. Strange, eds., *Handbook of Regional and Urban Economics*, Vol. 5 of *Handbook of Regional and Urban Economics*, Elsevier, 2015, pp. 405–465.

Kardan, Omid, Peter Gozdyra, Bratislav Misic, Faisal Moola, Lyle J. Palmer, Tomáš Paus, and Marc G. Berman, "Neighborhood greenspace and health in a large urban center," *Scientific Reports*, 2015, *5* (11610).

Kragh, J, "Road traffic noise attenuation by belts of trees," *Journal of Sound and Vibration*, 1981, *74* (2), 235–241.

Li, Zhao-Liang, Hua Wu, Si-Bo Duan, Wei Zhao, Huazhong Ren, Xiangyang Liu, Pei Leng, Ronglin Tang, Xin Ye, Jinshun Zhu et al., "Satellite remote sensing of global land surface temperature: Definition, methods, products, and applications," *Reviews of Geophysics*, 2023, *61* (1), e2022RG000777.

Lockhart, Brian Roy, Robert C Weih Jr, and Keith M Smith, "Crown radius and diameter at breast height relationships for six bottomland hardwood species," *Journal of the Arkansas Academy of Science*, 2005, *59* (1), 110–115.

MacFarlane, David W and Shawna Patterson Meyer, "Characteristics and distribution of potential ash tree hosts for emerald ash borer," *Forest Ecology and Management*, 2005, *213* (1-3), 15–24.

Manning, Sturt, Cindy Kocik, and et al. Sparks Jed, "Severe multi-year drought coincident with Hittite collapse around 1198?1196bc," *Nature*, 2023, *614*, 719–724.

Manoli, Gabriele, Simone Fatichi, Markus Schläpfer, Kailiang Yu, Thomas W Crowther, Naika Meili, Paolo Burlando, Gabriel G Katul, and Elie Bou-Zeid, "Magnitude of urban heat islands largely explained by climate and population," *Nature*, 2019, *573* (7772), 55–60.

Mohareb, Eugene A. and Adrian K. Mohareb, "A comparison of greenhouse gas emissions in the residential sector of major Canadian cities," *Canadian Journal of Civil Engineering*, 2014, *41* (4), 285–293.

Morales, Dominic J, "The contribution of trees to residential property value," *Journal of Arboriculture*, 1980, *6* (11), 305–308.

Mullaney, Jennifer, Terry Lucke, and Stephen J. Trueman, "A review of benefits and challenges in growing street trees in paved urban environments," *Landscape and Urban Planning*, 2015, *134*, 157–166.

Nikoofard, Sara, V. Ismet Ugursal, and Ian Beausoleil-Morrison, "Effect of external shading on household energy requirement for heating and cooling in Canada," *Energy and Buildings*, 2011, *43* (7), 1627 – 1635.

Nowak, David J and Eric J Greenfield, "Tree and impervious cover change in US cities," *Urban Forestry & Urban Greening*, 2012, *11* (1), 21–30.

_ **and** _ , "Declining urban and community tree cover in the United States," *Urban forestry & urban greening*, 2018, *32*, 32–55.

_ **and Tim Aevermann**, "Tree compensation rates: Compensating for the loss of future tree values," *Urban Forestry & Urban Greening*, 2019, *41*, 93–103.

_ **, Daniel E Crane, and Jack C Stevens**, "Air pollution removal by urban trees and shrubs in the United States," *Urban Forestry & Urban Greening*, 2006, *4* (3-4), 115–123.

Oke, T.R., "City size and the urban heat island," *Atmospheric Environment*, 1973, *7* (8), 769–779.

Peng, Shushi, Shilong Piao, Philippe Ciais, Pierre Friedlingstein, Catherine Ottle, François-Marie Bréon, Huijuan Nan, Liming Zhou, and Ranga B Myneni, "Surface urban heat island across 419 global big cities," *Environmental science & technology*, 2012, *46* (2), 696–703.

Pennisi, Elizabeth, "Forest giants are the trees most at risk," 2019.

Peper, Paula J., Claudia P. Alzate, John W. McNeil, and Jalil Hashemi, "Allometric equations for urban ash trees (Fraxinus spp.) in Oakville, Southern Ontario, Canada," *Urban Forestry & Urban Greening*, 2014, *13* (1), 175–183.

Popkin, Gabriel, "Deadly pest reaches Oregon, sparking fears for ash trees," *Science (New York, NY)*, 2022, *377* (6604), 356–356.

Price, Colin, "Quantifying the aesthetic benefits of urban forestry," *Urban Forestry & Urban Greening*, 2003, *1* (3), 123–133.

Rahman, Mohammad A., Yanin Pawijit, Chao Xu, Astrid Moser-Reischl, Hans Pretzsch, and Stephan Rötzer Thomas Pauleit, "A comparative analysis of urban forests for storm-water management," *Scientific Reports*, 2023, *13*, 1451.

Roy, Sudipto, Jason Byrne, and Catherine Pickering, "A systematic quantitative review of urban tree benefits, costs, and assessment methods across cities in different climatic zones," *Urban Forestry & Urban Greening*, 2012, *11*, 351–363.

Salmond, JA, DE Williams, G Laing, S Kingham, K Dirks, I Longley, and GS Henshaw, "The influence of vegetation on the horizontal and vertical distribution of pollutants in a street canyon," *Science of the total environment*, 2013, *443*, 287–298.

Santamouris, M., C. Cartalis, A. Synnefa, and D. Kolokotsa, "On the impact of urban heat island and global warming on the power demand and electricity consumption of buildings: A review," *Energy and Buildings*, 2015, *98*, 119–124. Renewable Energy Sources and Healthy Buildings.

Todorova, Assenna, Shoichiro Asakawa, and Tetsuya Aikoh, "Preferences for and attitudes towards street flowers and trees in Sapporo, Japan," *Landscape and urban planning*, 2004, *69* (4), 403–416.

Tucker, Compton, Martin Brandt, and et al. Fensholt Rasmus, "Subcontinental-scale carbon stocks of individual trees in African drylands," *Nature*, 2023, *615*, 80–86.

Tuholske, Cascade, Kelly Caylor, Chris Funk, Andrew Verdin, Stuart Sweeney, Kathryn Grace, Pete Peterson, and Tom Evans, "Global urban population exposure to extreme heat," *Proceedings of the National Academy of Sciences*, 2021, *118* (41), e2024792118.

Upreti, Ruby, Zhi-Hua Wang, and Jiachuan Yang, "Radiative shading effect of urban trees on cooling the regional built environment," *Urban Forestry and Urban Greening*, 2017, *26*, 18–24.

Wachter, Susan M. and Grace Wong, "What Is a Tree Worth? Green-City Strategies, Signaling and Housing Prices," *Real Estate Economics*, 2008, *36* (2), 213–239.

Willis, Katherine J and Gillian Petrokofsky, "The natural capital of city trees," *Science*, 2017, *356* (6336), 374–376.

Zhu, Pengyu and Yaoqi Zhang, "Demand for urban forests in United States cities," *Landscape and urban planning*, 2008, *84* (3-4), 293–300.

Zivin, Joshua Graff and Matthew Neidell, "Environment, Health, and Human Capital," *Journal of Economic Literature*, September 2013, *51* (3), 689–730.

For Online Publication

A Data appendix

This section complements Section 1 with: (i) a description of vegetation indices constructed from satellite imagery; (ii) an illustration of the dynamics of urban forestry over time using Google Street View; (iii) a description of transactions across neighborhoods of Toronto; and (iv) additional details about the construction of the energy data.

A.1 Satellite imagery

Our baseline specification relies on the land classification provided by the Urban Forestry services of the City of Toronto and based upon high-resolution satellite imagery and LiDAR information (City of Toronto, 2019). We however complement and validate these measures of land cover with low-resolution satellite imagery (Sentinel 2, 2016–2020, 10m resolution; Landsat L8, 2013–2020, 30m resolution; Landsat L7, 2007–2012, 30m resolution). One important benefit of using coarser, but more frequent, data is to shed light on the dynamics of tree cover over time (see Figure 3 in Section 1 for instance).

Figure A1. Satellite imagery and vegetation/built-up indices (2018).

(a) NDVI

(b) NDBI

Notes: This Figure displays vegetation against built-up indices, as constructed from a cloud-free mosaic of Sentinel imagery (S2, 10m resolution) covering May–September 2018 (North-East of Toronto). The Normalized Difference Vegetation Index (NDVI) is obtained by combining the reflection in the near-infrared spectrum (NIR) with the reflection in the red range of the spectrum (RED). The Normalized Difference Built-up Index (NDBI) is obtained by combining the reflection in the near-infrared spectrum (NIR) with the reflection in the short-wave infrared range of the spectrum (SWIR).

To construct vegetation, built-up and water indices, we proceed as follows for each collection of satellite imagery: (i) we isolate a summer period in any given year from June 1st to September 30th (to best capture vegetation); (ii) we construct a cloud-free mosaic of images taken during this period; (iii) we construct a set of indices, most notably, the Normalized Difference Vegetation Index (NDVI)—obtained by combining the reflection in the near-infrared spectrum (NIR) with the reflection in the red range of the spectrum (RED)—the Leaf Area Index (LAI), and the Normalized Difference Built-up Index (NDBI)—obtained by combining the reflection in the near-infrared spectrum (NIR) with the reflection in the short-wave infrared range of the spectrum (SWIR); and (iv) we construct the average indices within each postcode and every year covered by the collection. We illustrate the variation captured by NDVI and NDBI in Figure A1 (based on Sentinel S2 in 2018).

Figure A2. Validation of the measure of tree cover.

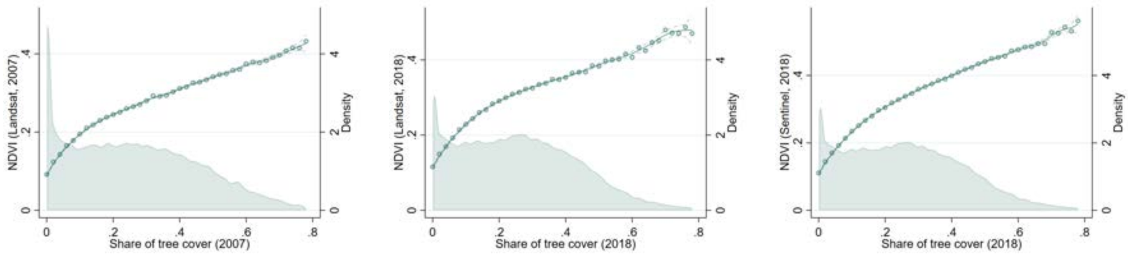

(a) NDVI (Landsat, 2007) (b) NDVI (Landsat, 2018) (c) NDVI (Sentinel, 2018)

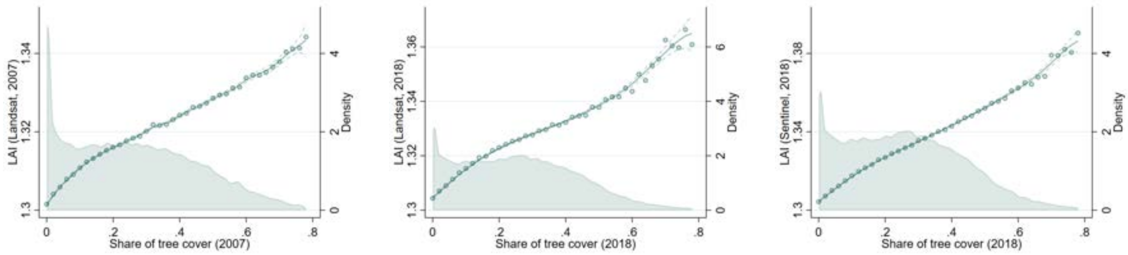

(d) LAI (Landsat, 2007) (e) LAI (Landsat, 2018) (f) LAI (Sentinel, 2018)

Notes: This Figure correlates the measure of tree cover produced by Urban Forestry as part of an Urban Tree Canopy (UTC) Assessment in 2007 and 2018 with standard vegetation indices extracted from recent satellite imagery. Panels (a), (b) and (c) correlate the area share of tree canopy in 2007 and 2018 with the Normalized Difference Vegetation Index (NDVI) across postcodes. The NDVI is obtained by combining the reflection in the near-infrared spectrum (NIR) with the reflection in the red range of the spectrum (RED). Panels (d), (e) and (f) correlate the share of tree coverage in 2007 and 2018 with the Leaf Area Index (LAI) across postcodes. The green area displays the distribution of the x-axis variable for each panel. Panels (a) and (d) rely on a cloud-free mosaic of Landsat imagery (L7, 30m resolution) covering May–September 2007. Panels (b) and (e) rely on a cloud-free mosaic of Landsat imagery (L8, 30m resolution) covering May–September 2018. Panels (c) and (f) rely on a cloud-free mosaic of Sentinel imagery (S2, 10m resolution) covering May–September 2018.

We use these indices to validate the land classification data and shed some light onto the dynamics of urban forestry over our period of interest. In Figure A2, we correlate the measure of tree cover produced by Urban Forestry as part of an Urban Tree Canopy (UTC) Assessment in 2007 and in 2018 with our vegetation indices, as extracted from recent satellite imagery (Landsat L7, Landsat L8, and Sentinel S2). We see that there is a very strong, positive, quasi-linear relationship between the area share covered by the tree canopy and the vegetation indices based on average reflectance across the visible, infra-red, near infra-red spectrum. These relationships are behind our findings of Section 1.3 where we show that a loss of 0.04-0.05 in the share of tree cover is accompanied by a decrease in the Normalized Difference Vegetation Index of 0.021 and in the Leaf Area Index of 0.0035. Figure A2 indeed shows that an additional 0.10 in tree cover corresponds to a 0.04 higher NDVI and a 0.005 higher LAI; a loss of 0.04-0.05 in tree canopy would thus be expected to decrease NDVI by 0.02 and LAI by 0.0025.

A.2 The dynamics of urban forestry over time

Google Street Views In Section 1.3 and Figure 3, we shed some light onto the swift decrease in vegetation cover experienced by neighborhoods with a high density of city-managed ash trees. We provide an illustration of the actual process of removal and replacement of city-managed trees in Figure A3. More specifically, we focus on the neighborhood depicted in Figure 2, James Park Square in Scarborough (North-East of Toronto), which experienced a massive loss in tree cover between 2007 and 2018 due to its row of city-managed ash trees.

Figure A3 presents successive street views of this neighborhood in 2007, 2014, and 2020. We see that the neighborhood is a typical leafy suburb in 2007, with individual homes, private gardens, and rows of city-managed (ash) trees. In 2014, the mature ash trees are already cut down and replaced by young sprouts, leading to a significant change in the visual appeal of the neighborhood and in shade coverage. In 2020, the substitute sprouts have grown into tree saplings, still short of providing any significant tree cover, shade or sheltering against wind. As argued in Section 1.3, the felling of mature trees induces a loss in tree canopy that cannot be mitigated within a span of 25-30 years.

The swift felling of ash trees and the distribution of injected trees In Figure 3 (Section 1.3), we show that most of the vegetation loss materializes between 2012–2016 in neighborhoods with high incidence of city-managed ash trees. We shed additional light on the swift felling of ash trees in Figure A4, where we exploit a specific dataset—distinct from the general register of city-managed trees—in which we do observe the planned removals of city-managed ash trees and the injections of TreeAzin between 2010 and 2014 (both ordered by the City of Toronto). We find that removals steadily increase between 2010 and the autumn of 2013, when the

Figure A3. The dynamics of urban forestry over time—an illustration using Google Street View.

(a) 2007

(b) 2014

(c) 2020

Notes: This Figure shows three snapshots of the neighborhood depicted in Figure 2 (James Park Square, Scarborough, North-East of Toronto)—with a relatively high density of ash trees at baseline. The images were extracted in 2007 (panel a, before the infestation), 2014 (panel b, after the cut-downs), and 2020 (panel c, with replanted tree saplings) from Google Maps.

monthly incidence of removals reaches about 1,000 ash trees. By contrast, TreeAzin injections are entirely concentrated in the months of June, July and August every year—when water and nutrients are most actively traveling upward through the

Figure A4. Removals and TreeAzin injections over time.

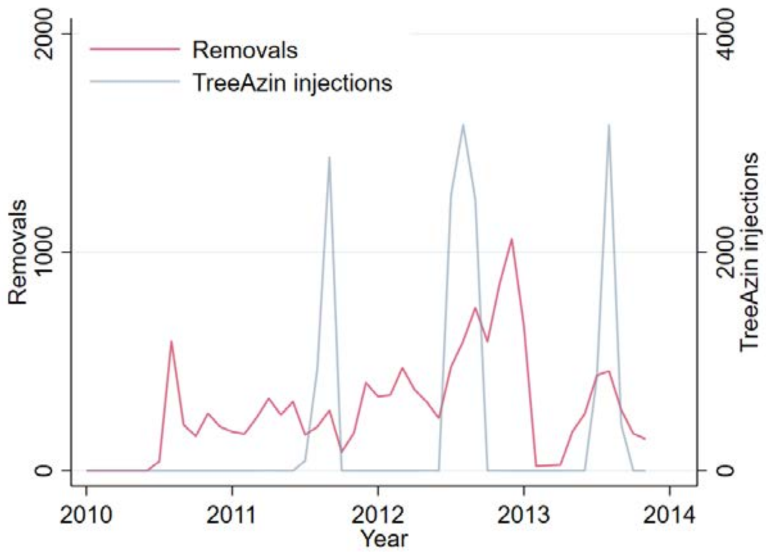

Notes: This Figure shows the evolution of tree removals and TreeAzin injections between 2010 and 2014. The data source is the register of ash trees—a specific sub-module distinct from the general register of city-managed trees that we use in our baseline analysis (see Table 1 for instance).

bark.

Analyzing the decision to save or remove a tree is complicated: we have limited evidence nor insight about the decision process or the constraints hinging on the Parks and Forestry department of the City of Toronto. We "quantify" the role of tree characteristics, the way they are planted, and their neighborhood in a variance-decomposition exercise where we regress removals/injections on: dummies for the exact tree species (e.g., red ash) and deciles of trunk diameters; dummies for the way they are planted (e.g, with pavers around the tree or as a container tree); and dummies for their ward. We find that tree characteristics explain 13% of the variance in whether the tree will be injected or removed; adding the planting structure explains 18%; and adding neighborhood fixed-effects explains 33%. In summary, geography and the age/species of the tree are the main predictors as to whether the tree will be saved or removed.

A.3 Transactions across neighborhoods

The transaction data used in Section 3 and described in Section 1.2 cover the whole City of Toronto from 2007 to 2017. Note that we also have transaction data from 2002 to 2006—used in a robustness check—, but without detailed dwelling characteristics.

Figure A5. Transactions and their average price across the City of Toronto.

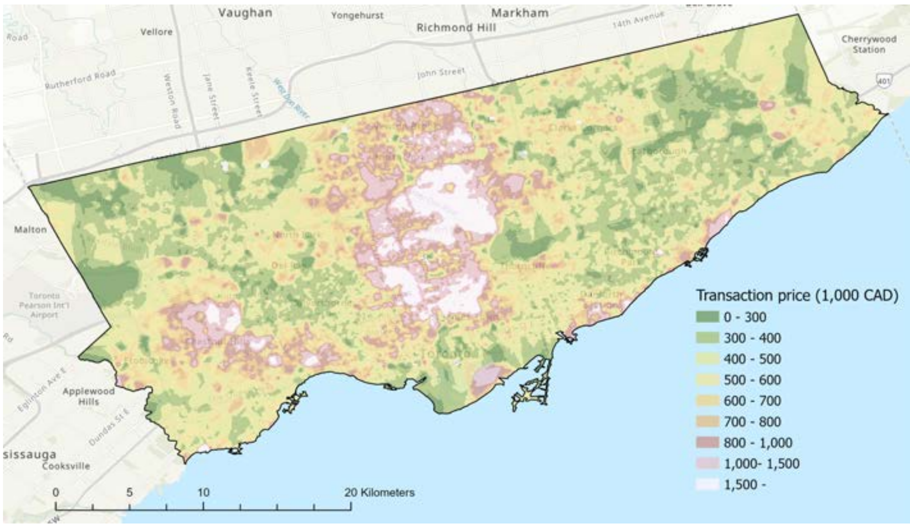

(a) Average transaction price

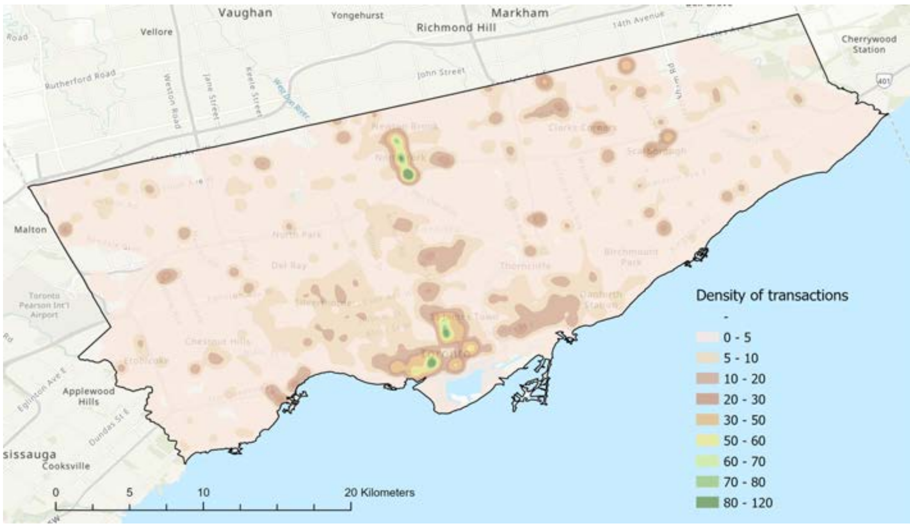

(b) Number of transactions

Notes: Panel (a) shows the average transaction price for all transactions between 2007 and 2017 in 1,000 CAD (from green to yellow to pink and then white, as standard in an elevation scale). One can see that the stretch between Yorkville and North York, Chestnut Hills (West of Toronto), and a few coastal neighborhoods are the neighborhoods with the highest transaction prices. Panel (b) displays the geography of property transactions between 2007 and 2017 across the City of Toronto. Each color class represents a bin of density (from white to pink to yellow and then green, as an inverted elevation scale). Note that the density is obtained through a kernel density procedure such that the scale does not have an easily-interpretable unit.

We illustrate the geography of the housing market in Figure A5, where we display the average transaction price for all transactions between 2007 and 2017 in panel (a) and the density of transactions in panel (b). One can see that a few neighborhoods are highly demanded, most notably the area between Bloor-Yorkville and North York. This area is quite green, traversed by ravines, as shown in Figure 1. The correlation between transaction prices and the density of city-managed ash trees is however unclear at the neighborhood level: the neighborhoods of Mount Pleasant, North York, Scarborough (East), and Etobicoke are the ones with the highest density of ash trees, but while the former two are quite demanded, Etobicoke is less demanded and Scarborough is considered a relatively deprived area (compared to the rest of the City of Toronto).

Figure A6. The cooling effect of urban forestry—an illustration during the heatwave in 2018.

(a) NDVI

(b) Land Surface Temperature

Notes: This Figure exploits Landsat 8 satellite imagery in July and August 2018. The left panel shows the Normalized Difference Vegetation Index (NDVI) where green colors indicate a higher vegetation cover. The right panel shows the Land Surface Temperature (LST) where red colors indicate higher temperatures.

A.4 Tree canopy and temperature

In Section 4, we discuss the cooling effect of the tree canopy during heatwaves. Figure A6 further illustrates the correlation between urban temperature and urban forestry. We construct an average mosaic of Landsat 8 satellite imagery in July and August 2018 and consider two indices based on the relative reflectance of different bands: the Normalized Difference Vegetation Index (NDVI) capturing vegetation cover; and the Land Surface Temperature (LST) which we also calculate at a 30-meter spatial resolution.[17] The left panel of Figure A6 displays the average Normalized Difference Vegetation Index over the period, and the right panel shows the average Land Surface Temperature across two adjacent neighborhoods with significant differences in tree canopy coverage (South Parkdale, South-West of Toronto).

[17]As mentioned in section A, the two measures share some small, mechanical correlation because the LST calculations employ a fractional vegetation measure that is based on the ratio of the maximum and minimum values of the NDVI to correct the temperature measure derived from the Thermal Infrared (TIRS) band (see Ermida et al., 2020; Li et al., 2023, for more details).

We observe a sharp difference between the West and the East of Dufferin St: the tree coverage in the West of Dufferin St markedly alleviates the rise in temperature during this heat wave episode.

Figure A7. The cooling effect of urban forestry—a map of Toronto during the heatwave in 2018.

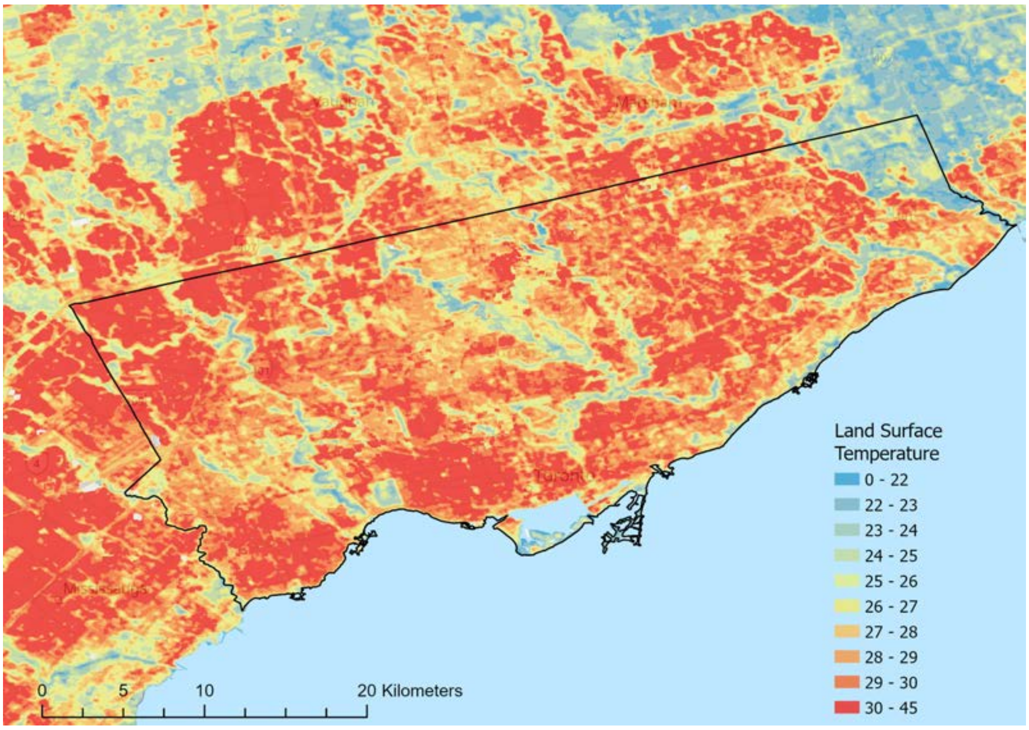

Notes: This Figure displays the average Land Surface Temperature (LST) across the City of Toronto during July and August 2018.

We shed additional light on the urban heat island effect and the role of urban forestry in Figure A7, where we display the Land Surface Temperature (LST) for the months of July and August 2018 across the City of Toronto and its immediate hinterlands. There are two salient observations. First, there is a very significant temperature differential (of the order of magnitude of 5 degrees) between the city and its hinterlands. This is within the interval of urban island effects estimated in Manoli et al. (2019) across many cities of the developed and developing World. Second, there is some variation within neighborhoods of the City of Toronto: for instance, one can distinctly see the temperature gradient between the numerous ravines, forming a large ravine system and hosting a dense urban forest, and the impervious areas surrounding those ravines.

A.5 Energy consumption

In the raw data, energy consumption is reported in kilowatt hours (kWh) adjusted for line losses over the billing period. The days of service in a billing period range between 1 and 2 months (see Figure A8) and we know the start and end date of each billing period which varies across households. To calculate the statistics about energy consumption in postcode p, month m and year t, we construct a daily panel of each household i's average daily energy consumption and estimate:

$$e_{ipmt} = \alpha_i + E_{pmt} + \epsilon_{ipmt}$$

where the fixed effects E_{pmt} capture the average daily energy consumption in postcode p for a given month m of year t. To derive a measure e_{pmt} of the average energy consumption per month and year, we multiply the average daily energy consumption e_{ipmt} by the number of days in the respective month m. One nice feature of our electricity data is that we can condition the estimation on energy meter fixed effects, α_i, which absorb all time-invariant house and occupant characteristics. The latter control, for example, for the energy efficiency of the house.

Figure A8. Distribution of the days of service intervals across billing periods.

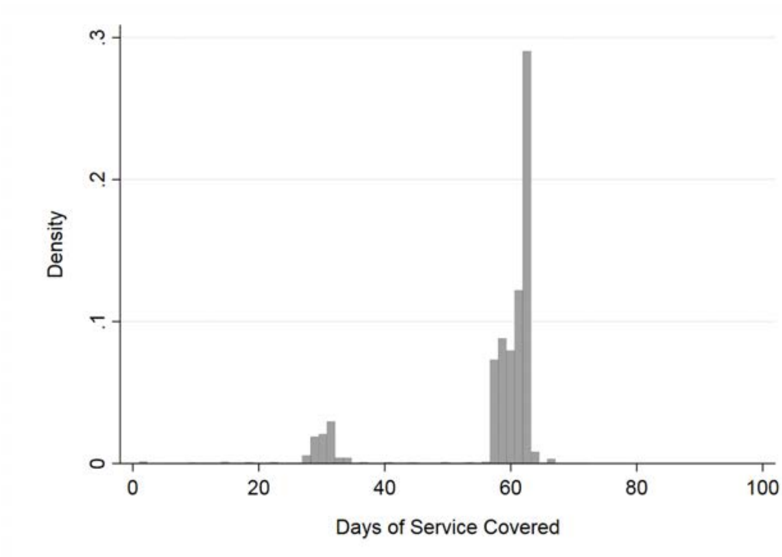

Notes: This Figure represents the distribution of the days of service intervals across billing periods and is based on residential energy meters between 2011 and 2021.

There are important seasonal patterns in energy consumption which we illustrate in Figure A9. Electricity consumption is high in the summer months, due to the use of air conditioning. Between November–April, electricity consumption is a mix of light and electrical heating, even though natural gas is the most common source of heating fuel. Consequently, we would expect trees to have more pronounced electricity consumption effects in the summer. Natural gas is used for heating during these winter months and there is indeed a significantly higher usage of natural gas in these months with a spike in January and February, the coldest months.

Figure A9. Electricity and gas consumption over time.

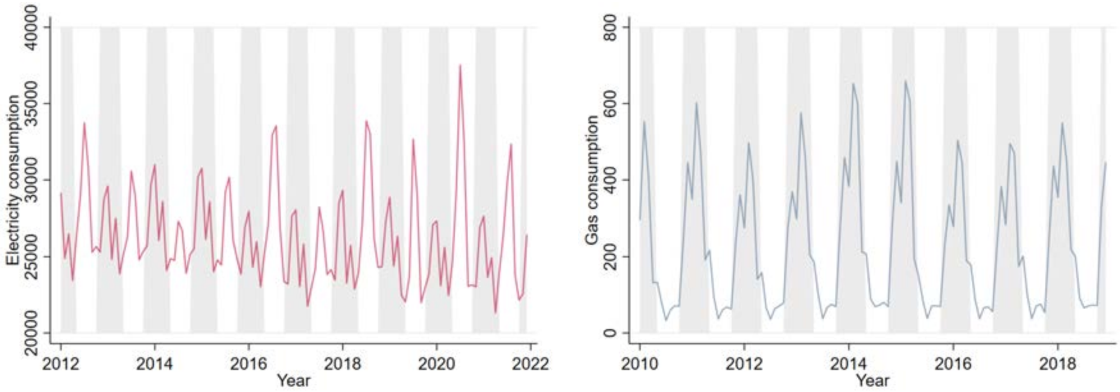

(a) Electricity (b) Natural gas

Notes: The left panel of the graph shows the adjusted monthly electricity consumption measured in kWh across postcodes in Toronto. The right panel shows the average monthly consumption of natural gas measured in cubic meters across postcodes in Toronto. Gray shaded areas indicate winter months, i.e., November–April.

B Neighborhood segregation and the heterogeneous value of trees

This section sheds some light onto the unequal distribution of urban forestry and the possibly heterogeneous value of urban trees.

Figure B1. Deprivation and density of the tree canopy.

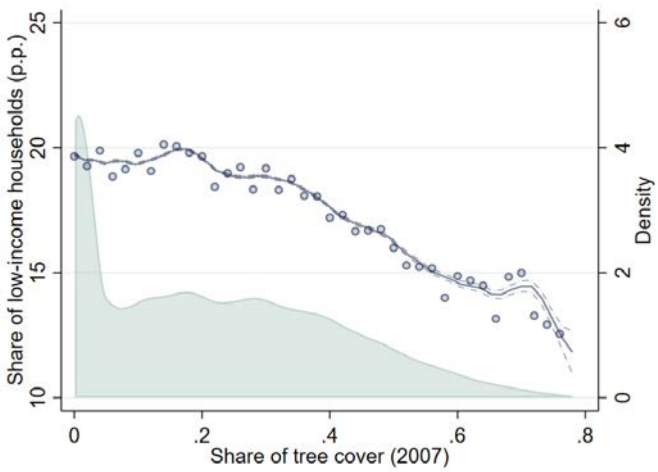

Notes: This Figure represents the relationship between the share of low-income households at the neighborhood level and our measure of tree cover at the postcode level. We group transactions by bins of tree cover: the dots represent the average share of low-income households within each bin. The green area represents the distribution of the x-axis variable across all panels. The lines are locally weighted regression on all observations.

B.1 The unequal distribution of urban forestry

The distribution of urban forestry is unequal across space, as documented in Section 1. The prevalence of trees interacts with neighborhood characteristics in a systematic manner. We illustrate the inequalities in access to urban trees in Figure B1 where we correlate the density of the local tree canopy with a deprivation measure, i.e., the share of low-income households. We find that the average share of low-income households is around 20% in neighborhoods without any tree versus 12% in the leafiest postal codes.

B.2 The heterogeneous value of (the marginal) trees

The unequal distribution of urban forestry could illustrate the heterogeneous value of (the marginal) trees: trees might be highly valued in richer, less densely-populated neighborhoods with larger properties. In such a context, they might have higher aesthetic value (Benson et al., 1998; Price, 2003; Todorova et al., 2004) and better complement the "consumption of the public space" by residents.

Table B1. The amenity value of trees—heterogeneous treatment effects.

Transaction price (log)	(1)	(2)	(3)
Tree cover	1.047	-0.109	0.867
	(0.306)	(0.456)	(0.305)
Tree cover × Deprived	-0.420		
	(0.346)		
Tree cover × Green		1.015	
		(0.510)	
Tree cover × House			-0.001
			(0.088)
Transaction controls	Yes	Yes	Yes
Observations	374,286	374,286	374,286
F-statistic	42.98	21.58	41.38

Notes: Standard errors are reported between parentheses and are clustered at the postcode × year level. All specifications report the estimates from IV specifications in which tree cover and its interaction with different variables are instrumented by the the density of city-managed ash trees and the interacted instrument. The unit of observation is a transaction, and the dependent variable is the (log) transaction price. All specifications are weighted by the inverse of the number of observations in a given postcode and include the following controls: (i) postcode fixed effects; (ii) ward fixed effects interacted with year fixed effects; (iii) a measure of city-managed tree density interacted with year fixed effects; (iv) latitude and longitude interacted with year fixed effects; (v) area shares from the land classification in 2007 (tree canopy, grass/shrub, bare earth, water, buildings, roads, other paved surfaces and agriculture) interacted with year fixed effects; and the number of washrooms and bedrooms interacted with year fixed effects. *Deprived* is a dummy equal to 1 if the share of low-income household is above 20% within the neighborhood. *Green* is a dummy equal to 1 if the area share of trees is above median (across postal codes) in 2007. *House* is a dummy equal to 1 if the transaction is labeled as "Low Density Residential", i.e., not within multi-unit buildings.

We evaluate the heterogeneous treatment effects of trees on transaction prices in Table B1 where we interact our treatment with a measure of deprivation—a dummy equal to 1 if the share of low-income household is above 20% within the neighborhood—, a measure of greenness—a dummy equal to 1 if the area share of trees is above median (across postal codes) in 2007—and a dummy equal to 1 if the transaction is not within multi-unit buildings. We find that the treatment effect is larger in richer areas: one additional percentage point in tree cover within a postcode increases property prices by 1.05% in non-deprived neighborhoods versus 0.62% in deprived neighborhoods (column 1). The treatment effect is entirely explained by postal codes that were originally quite green (column 2). Finally, there is no premium associated with the type of transactions: multi-unit buildings command the same premium as individual houses in leafy suburbs (column 3).

We further study the non-linear effects of the tree canopy on temperature and electricity consumption during July and August in Table B2. The table reports

Table B2. The non-linear value of trees.

	Land Surface Temperature	Electricity consumption (log)
Tree cover	-7.469	-3.798
	(3.390)	(0.649)
Tree cover × Initial	1.254	0.892
	(1.366)	(0.119)
Observations	702,138	280,931
F-statistic	59.47	101.25

Notes: Standard errors are reported between parentheses and are clustered at the postcode × year level. All specifications report the estimates from IV specifications in which tree cover and its interaction with the (standardized) area share of tree cover in 2007 are instrumented by the the density of city-managed ash trees and the interacted instrument. The unit of observation is a postal code in a given year. In column (1), the dependent variable is the Land Surface Temperature (LST) computed as an average during July/August. In column (2), the dependent variable is the (log) electricity consumption in July/August for the median household within a postal code and for all years between 2012–2020. All specifications are weighted by the inverse of the number of observations in a given postcode and include the following controls: (i) postcode fixed effects; (ii) ward fixed effects interacted with year fixed effects; (iii) a measure of city-managed tree density interacted with year fixed effects; (iv) latitude and longitude interacted with year fixed effects; (v) area shares from the land classification in 2007 (tree canopy, grass/shrub, bare earth, water, buildings, roads, other paved surfaces and agriculture) interacted with year fixed effects. In column (2), we omit postcode fixed effects.

the estimates from a two-stage specification in which tree cover and its interaction with the (standardized) area share of tree cover in 2007 are instrumented by the density of city-managed ash trees and the interacted instrument. In other words, the coefficient in front of the interaction can be understood as the impact of an additional standard deviation in initial tree cover on the treatment effect.

We find moderate non-linearities in the cooling effect of the marginal tree. On average, one additional percentage point in tree cover within a postcode reduces temperature by about 0.05 degrees (see Panel A of Table 5); a standard deviation in initial tree cover would reduce this effect by 0.01 degrees (see column 1 of Table B2). These non-linearities translate into moderate non-linearities in the energy-saving effect of the marginal tree: one additional percentage point in tree cover within a postcode reduces electricity consumption by 2.5% (see Panel B of Table 5); a standard deviation in initial tree cover would reduce this effect by 0.9% degrees (see column 2 of Table B2). Interestingly, the direction of this treatment heterogeneity goes opposite to that found for the hedonic value of urban forestry in Table B1.

C Tree canopy and energy consumption

This section provides complements to Section 4. More specifically, we highlight the time-varying effect of the ecological catastrophe on neighborhoods with high density of city-managed ash trees, and we analyze this effect for Land Surface Temperature between 2006–2018 and electricity consumption (during summer) between 2012–2020. We also provide a "placebo" test analyzing the relationship between urban forestry and electricity consumption during winter. We leverage episodes of high temperatures (resp. wind chill) to estimate the energy-consumption effect of urban forestry as a function of the solar-shading potential (resp. wind-sheltering potential) of the local urban forestry. Lastly, we provide details behind our decomposition exercise (see "The quantitative role of energy savings" in Section 4).

Figure C1. The ecological catastrophe and the cooling effects of tree canopy over time.

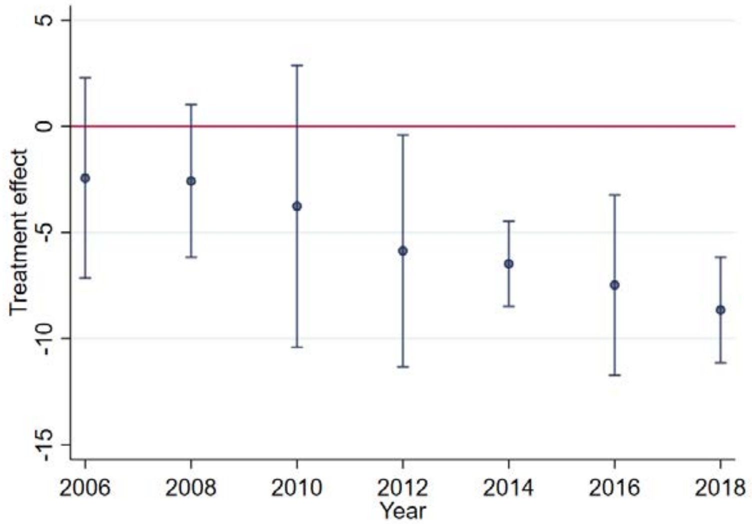

Notes: This Figure shows the estimated correlation between tree density and Land Surface Temperature (LST) for the months of July and August for each year between 2006 and 2018 (see Equation 4). More specifically, we regress the Land Surface Temperature (for a group of two consecutive years, τ) across postcodes on the measure of tree cover in 2018, instrumented by the number of street ash trees per area within a 10m buffer (as measured in 2010). We control for a measure of street tree density, ward fixed effects, latitude, longitude, and dummies for the land classification in 2007 (tree canopy, grass/shrub, bare earth, water, buildings, roads, other paved surfaces and agriculture). The reported coefficients are the ones in front of the measure of tree density, and vertical lines show 95 percent confidence intervals.

C.1 Temperature and energy consumption effects over time

Temperature effects over time We consider the following specification to isolate the time-varying effects of the Emerald Ash Borer infestation (through its impact on the tree canopy),

$$T_p^\tau = \alpha + \beta^\tau TD_{p,2018} + \gamma \mathbf{X}_p + \eta_w + \varepsilon_p, \tag{4}$$

where each observation is a postal code, T_p^τ is the average Land Surface Temperature within postcode p during July and August of a year τ, and urban forestry in 2018, $TD_{p,2018}$, is instrumented by the density of ash trees at baseline, $A_{p,2010}$. Controls include ward fixed effects η_w, latitude and longitude, the density of publicly maintained trees, and area shares from the land classification in 2007. We estimate β^τ separately for each year τ and report the estimates with their confidence intervals in Figure C1.

Intuitively, the estimates presented in Figure C1 are the causal effects of the catastrophe in each year, mitigated through the evolution of the tree canopy, i.e., the exercise can be loosely interpreted as an event-study design. Figure C1 shows that the impact of the infestation starts to materialize after 2010. In 2018, a 10 percentage point additional tree cover within a postcode reduces temperature by about 0.8 degrees (Celsius). In theory, the gradient in the treatment effect could reflect two forces: (i) the tree felling is gradually implemented across the City of Toronto—as illustrated in Section 1.3—thus inducing higher treatment compliance over time; and (ii) there are secular trends in summer temperatures due to climate change.

Energy consumption over time and across seasons We replicate the exercise of Figure C1 and Equation (4) for average energy consumption across the summer months (July and August) in panel (a) of Figure C2. Note that, in contrast with Figure C1, we do not observe electricity consumption before the start of the ecological catastrophe such that all years should be considered "treated", at least to some extent. We find a small gradient in energy consumption from 2012–2014 and a subsequent stabilization of the effect. In panel (b) of Figure C2, we look at electricity consumption as the dependent variable of Equation (4), but we calculate it for the winter months (December to February). We consider this specification as a placebo test: the evolution of the tree canopy—as triggered by the ecological catastrophe—should matter most during summer. Panel (b) of Figure C2 indeed finds a more limited correlation between urban forestry and electricity saving during winter.

Figure C2. The ecological catastrophe and its energy consumption effects over time.

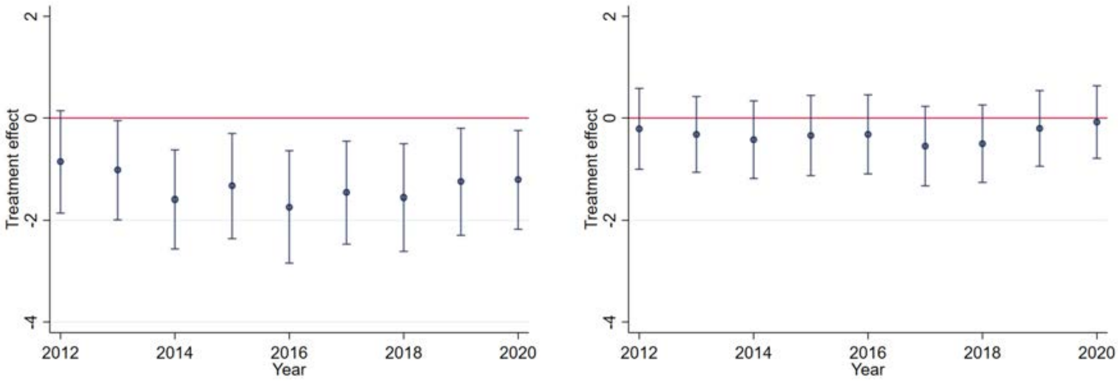

(a) July-August (2012–2020) (b) December-February (2012–2020)

Notes: Panel (a) shows the estimated correlation between tree density and electricity consumption for the months of July and August for each year between 2012 and 2020 (see Equation 4). More specifically, we regress the (log) electricity consumption across postcodes on the measure of tree cover in 2018, instrumented by the number of street ash trees per area within a 10m buffer (as measured in 2010). We control for a measure of street tree density, ward fixed effects, latitude, longitude, and dummies for the land classification in 2007 (tree canopy, grass/shrub, bare earth, water, buildings, roads, other paved surfaces and agriculture). The reported coefficients are the ones in front of the measure of tree density, and vertical lines show 95 percent confidence intervals. Panel (b) replicates the exercise for winter months (December to February).

C.2 Construction of the shade and shelter measures

In this section, we focus on the construction of two measures, the *solar-shading potential* and the *wind-sheltering potential*, which underlie our alternative empirical strategy based on the orientation of trees around homes.

For the shading potential of the neighboring tree canopy, we compute the measure S_{iw} for property i and week w of a given year as,

$$S_{iw} = \frac{\int Sun_{w\tau} \times Shade_{iw\tau} d\tau}{\int Sun_{w\tau} d\tau},$$

where τ is a time of the day (in practice, we divide the day into discrete intervals of 15 minutes), $Sun_{w\tau}$ is the potential sun exposure at time τ in week w , and $Shade_{iw\tau}$ is a measure of shade induced by the presence of trees around property i at time τ in week w. The variable $Shade_{iw\tau}$ is constructed by reconstituting the week-specific solar angle $a_w(\tau)$ and sun direction $\theta_w(\tau)$ as a function of time τ. At time τ, we select all trees in direction $\theta_w(\tau)$ originating from the centroid of a property. We then calculate the share of the property which is in the shade of these trees, $Shade_{iw\tau}$, exploiting the distance to the trees and the solar angle. This computation requires several assumptions regarding the height of a tree, the diameter of its crown, and the height of a property. We provide additional details about the computation

Figure C3. Shading effect of trees as a function of the time of the day and week.

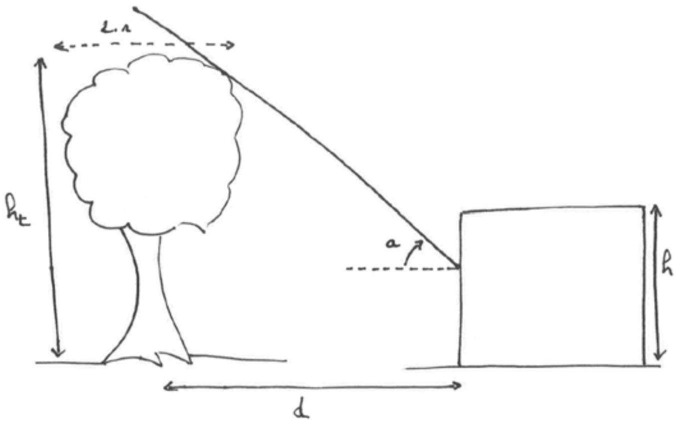

Notes: This Figure schematically represents the parameters used to derive the measure $Shade_{iw\tau}$, which depends on a week of the year w, a time of the day τ (a discrete interval of 15 minutes), and the surroundings of property i. We calculate the shade, $Shade_{iw\tau}$, as follows. At a given time of the day τ in week w, we identify the direction of the sun (in degrees, e.g., North would be 90 degrees) and the associated sun angle a. For instance, the sun angle would be generally lower during winter, and temporarily lower early in the day (when the direction is around 0 degrees) or late in the afternoon (when the direction is around 180 degrees). We then calculate the percentage of the house front covered in shade by the nearest tree (distance d) in the identified direction. This simplification allows us to ignore the trees behind this closest tree and to abstain from calibrating an imperfect shading provided by trees. For this exercise, we consider a house front to be between 2 and 7 meters, and we assume that trees are $h_t = 20$ meters high with a crown radius of $r = 5$ meters—both parameters being probably on the higher end of the tree size distribution. As apparent from the Figure, the percentage of the house front covered in shade is a simple function of the sun angle a, the height of the house, the distance to the tree, and the tree dimensions.

in Figure C3. Note that we aggregate the property-specific measure, S_{iw}, into an average postcode measure, S_{pw}.

Figure C4. Sheltering effect of trees.

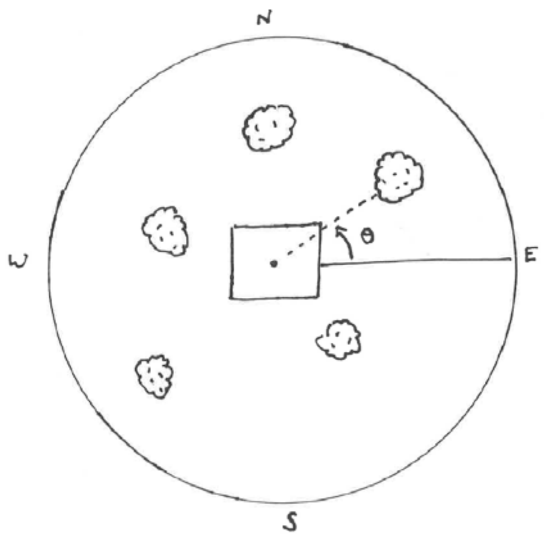

Notes: This Figure schematically represents the parameters used in order to derive the measure $Tree_{\theta i}$ used to construct the sheltering effect of trees. We combine the surroundings of property i with the direction of wind θ as follows: $Tree_{\theta i}$ is a dummy equal to 1 if there is a tree in direction θ and within 20 meters of the property.

To capture the sheltering potential of trees in the vicinity of property i in week w of a given year, we compute

$$W_{iw} = \sum_{\theta=0}^{360} w_{\theta w}(1 - Tree_{\theta i})p_{\theta t},$$

where: $w_{\theta w}$ is the Wind Chill Equivalent Temperature (WCET) used by Environment Canada, accounting for the average wind speed from direction θ (Celsius degrees); $Tree_{\theta i}$ is a dummy equal to 1 if there is a tree in direction θ and within 20 meters of the property; and $p_{\theta t}$ is the probability that the wind originated from direction θ in week w. We also compute a counterfactual measure for the Wind Chill Equivalent Temperature (WCET), ignoring the neighboring urban forestry:

$$W_{iw}^{c} = \sum_{\theta} w_{\theta w} p_{\theta w}$$

In other words, any difference between W_{iw} and W_{iw}^{c} has to relate to the distribution of urban forestry. We illustrate the simple intuition behind the construction of measure W_{iw} in Figure C4. We finally aggregate the property-specific measures, (W_{iw}, W_{iw}^{c}), into average postcode measures, (W_{pw}, W_{pw}^{c}).

C.3 Shade, shelter, and energy consumption

Empirical strategy To estimate the (local) cooling effect of urban forestry, we rely on a different empirical specification from that of the baseline strategy and rather exploit short-run fluctuations in weather conditions. We run a simple difference-in-differences specification at the postcode level for all weeks w in year t between January 2011 and December 2015. Letting p denote a postcode, w a week and t a particular year, we estimate the following equation:

$$\ln(E_{pwt}) = \alpha + \beta_2 S_{pw} \times Temp_t + \beta_1 S_{pw} + \beta_0 Temp_t + \delta_p + \nu_w + \mu_t + \varepsilon_{pwt}, \tag{5}$$

where E_{pwt} is a measure of energy consumption in a postcode/date, the measure S_{pw} captures the shade induced by surrounding trees in week w, thus depending on seasonal solar angles, and the measure $Temp_t$ is a dummy equal to 1 during episodes of exceptionally high temperatures (within the top decile between May and September). The identification of the parameter β_2 reflects excess energy savings during extreme weather episodes in properties with higher *solar-shading potential*. The set of fixed effects ν_w and μ_t capture seasonality and trends in energy consumption; these fixed effects can also be interacted to clean for average consumption within a given week and isolate the (lower) excess consumption for properties surrounded by trees.

We run a similar regression during low-temperature episodes in order to estimate the wind-sheltering effect of urban forestry.[18] Letting p denote a postcode, w the week, and t the year, we estimate the following equation:

$$\ln(E_{pwt}) = a + bW_{pwt} + cW^c_{pwt} + \delta_p + \nu_w + \mu_t + \varepsilon_{pwt}, \tag{6}$$

where the measures W_{pt} and W^c_{pt} are measures of wind chill—W_{pt} accounting for the presence of surrounding trees and prevailing wind directions at that date. The identification of parameter b reflects excess energy savings during extreme (cold) weather episodes in properties with higher *wind-sheltering potential*. As before, ν_w and μ_t are week and year fixed effects that may also be interacted.

Figure C5. Excess energy consumption in extreme weather episodes and the relative positioning of trees.

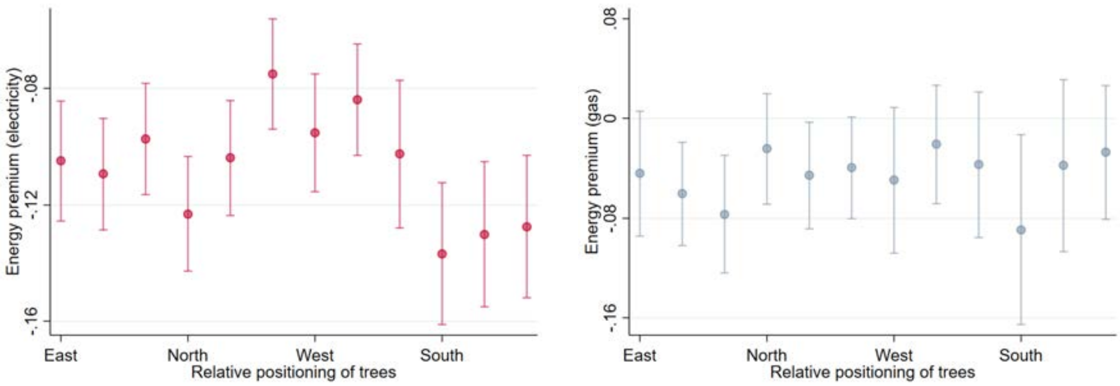

(a) Heat waves (b) Wind chill

Notes: This Figure represents the conditional correlations between energy consumption and the presence of trees in different directions from the average property within a postal code. Panel (a) reports the correlations between energy consumption and a dummy for heat waves interacted with the average number of trees within 10 meters for all houses of a given postal code in given directions (discretized between 0 and 360 degrees, with 30-degree intervals). Panel (b) reports the correlations between energy consumption and a dummy equal to 1 if the wind chill equivalent temperature is lower than 0 Celsius degrees during a given week interacted with the average number of trees in a certain direction across all houses of the postal code (East, North, West, South, every 30 degrees).

Shade and energy consumption We now quantify the energy-saving effect of trees. For illustrative purposes, we will use figures to show our main findings, and we leave the underlying regression models to Tables C1 and C2. Panel (a) of Figure A9 describes the relationship between excess energy consumption during heat waves and

[18]Since 70 percent of energy used in the residential sector comes from oil or gas (Mohareb and Mohareb, 2014), we expect a stronger effect of wind-sheltering on gas consumption. However, some heating is electric and we still expect to find some effect.

the relative positioning of trees. We estimate the conditional correlation between excess energy consumption and surrounding trees as follows. We regress the postcode energy consumption on a dummy for heat waves, the average number of trees within 10 meters for all houses of a given postal code in a certain direction and their interaction, while controlling for time-fixed effects and postcode fixed-effects. Figure A9 reports the energy premium guaranteed by the presence of trees during heat waves (the interaction term), conditional on a given direction (discretized between 0 and 360 degrees, with 30-degree intervals). As apparent, the energy premium associated with the presence of a tree is not negligible. The premium is significant across all directions, but even more so in the East and South where shade is likely to provide cooling. For instance, one additional tree for all houses of a given postal code—within 10 meters of each house and oriented South—is associated with a 14% decrease in energy consumption during heatwaves. One additional tree towards the North-West is associated with a 8% decrease in energy consumption.

Table C1. Energy consumption and the cooling effect of trees.

Energy consumption	(1)	(2)	(3)
Heat wave	.1073	.0437	.0437
	(.0137)	(.0109)	(.0109)
Heat wave × Shade	-.2997	-.3154	-.3157
	(.0518)	(.0528)	(.0528)
Observations	2,271,628	2,271,628	2,271,628
Fixed effects (postcode)	No	Yes	Yes
Fixed effects (time)	Year	Week/year	Week/year
Controls (historical temperature)	No	No	Yes

Standard errors are reported between parentheses and are clustered at the date-level. The unit of observation is a date × postcode.

Table C1 reports the estimates from Equation (5). We find that heat waves increase energy consumption, but less so in neighborhoods with high average shading potential across houses. More specifically, consumption increases by about 11% in postal codes without trees and this premium reduces to $0.11 - 0.26 \times 0.30 \approx 3\%$ for neighborhoods within the highest percentile of shade potential (0.26).

Sheltering effect and energy consumption Panel (b) of Figure A9 sheds light on the role of urban forestry during episodes of extreme cold. We regress the average energy consumption within a postal code on a dummy equal to 1 if the wind chill equivalent temperature is lower than 0 Celsius degrees during a given week, the average number of trees in a certain direction across all houses of the postal code (East, North, West, South, every 30 degrees), and their interaction, while controlling for time-fixed effects and postcode fixed-effects. The energy premium associated with the presence of a tree is smaller than it is for extreme heat episodes: on average, a tree in the path of the wind reduces energy consumption by 5% during weeks of frosty episodes. The estimated effect is not consistently (significantly) different from 0 across all directions: it is higher when winds originate from the South/East, possibly because such winds create a phenomenon called " lake-effect snow".[19] One additional tree for all houses of a given postal code—within 10 meters of each house and oriented South-East—is associated with a 8% decrease in energy consumption during cold waves.

Table C2. Energy consumption and the sheltering effect of trees.

Energy consumption	(1)	(2)	(3)
Wind chill (no shelter)	-.0047	-.0039	-.0038
	(.0004)	(.0005)	(.0005)
Wind chill (shelter)	.0015	.0016	.0016
	(.0003)	(.0003)	(.0003)
Observations	2,161,759	2,161,759	2,161,759
Fixed effects (postcode)	No	Yes	Yes
Fixed effects (time)	Year	Week/year	Week/year
Controls (historical temperature)	No	No	Yes

Standard errors are reported between parentheses and are clustered at the date-level. The unit of observation is a date × postcode. *Wind chill* is a measure of felt temperature accounting for wind speed (and shelter in the second row).

Table C2 reports the estimates from Equation (6). We find that a decrease of one degree (Celsius) during winter increases the weekly energy consumption by 0.4% for neighborhoods without urban forestry. The presence of a "blocking tree" in the path of the wind for all houses within the postal code reduces this effect to 0.22%. These effects are markedly lower than the cooling effects of urban forestry during summer, as discussed in the next section.

C.4 The quantitative role of energy savings

This section provides complements to the sub-section entitled "The quantitative role of energy savings" in Section 4.

[19] Note that prevailing winds in Toronto blow from the West, sometimes from the South or North, but more rarely from the East.

Energy savings and the amenity value of urban forestry Panel B of Table 5 shows that one percentage point in the area share of urban forestry reduces the average electricity consumption within a postal code by about 2.5%. This effect is however confined to two months in July and August; and the tree-saving effect is much lower during other times of the year. For instance, Figure C2 shows that the effect is about six-seven times lower during winter. Based on these causal estimates, we consider that one additional percentage point in tree cover reduces energy consumption by 0.4% through its cooling effect, and by 0.1% through its wind-sheltering properties—both effects being here smoothed over a period of 12 months. Considering that the average monthly expenditure in our sample is around CAD 200 in 2018, those cumulative effects would amount to CAD 1 per month. In comparison, the associated increase in the flow value of a property of 0.86% would correspond to CAD 21 per month—a calculation based on the fact that the average monthly rent for a two-bedroom apartment was around CAD 2,500 in 2018.

Energy savings and maintenance costs The previous calculations are nested at the level of a household. In order to compare the energy benefits of urban forestry with its maintenance costs, we need to aggregate those effects at the level of the City of Toronto. We also need to convert the cover in urban forestry into a number of trees.

First, please note that adding one tree within a postcode increases the area share of tree canopy by 0.45 percentage points (a calculation that we explain in Section 1.3); this 0.45 is the conversion rate that we will use thereafter. Second, from the previous calculations, adding a tree lowers the *annual* energy consumption by CAD $12 \times 1 \times 0.45 \approx 5.40$ *for each household*. With about 20 households per postcode, the total energy-saving benefit of a tree is thus CAD 108 per year. Ignoring the opportunity costs of land usage, such energy benefits would be *much* larger than the maintenance costs of urban forestry (estimated at around CAD 4.20 in the 2011 City of Toronto Parks and Forestry budget proposal).

Energy savings in a changing climate With a non-linear relationship between temperature and energy consumption, there should be an increasing impact of urban forestry on energy savings over time—owing to the marked increase in the expected occurrence of heat waves.

We illustrate the non-linear relationship between temperature and energy consumption in Figure C6 where we leverage weekly data on electricity consumption between 2012 and 2020, which we match with maximum weekly temperature. We

Figure C6. Electricity consumption and weekly temperature.

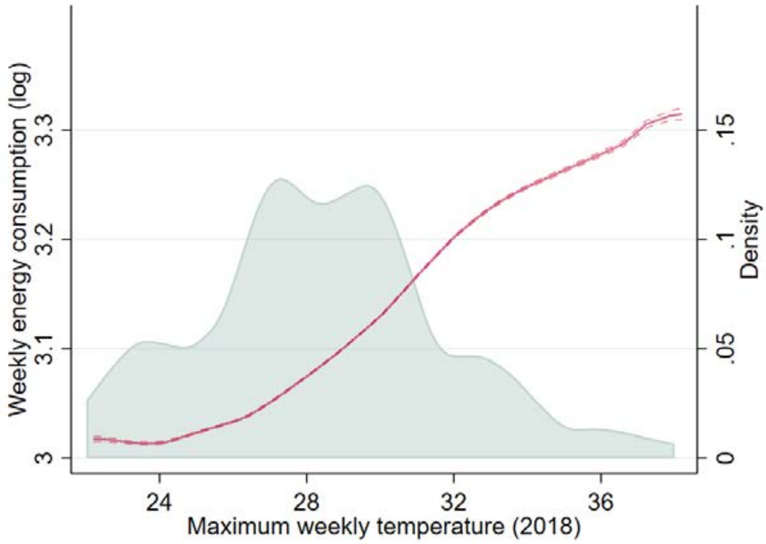

Notes: This Figure represents the relationship between the (weekly) energy consumption and the maximum weekly temperature. We group weeks by bins of weekly temperature: the dots represent the average energy consumption within each bin. The green area represents the distribution of the x-axis variable; and the sample is confined to summer months (July and August).

find that an increase of temperature from 23 degrees (Celsius) to 24 degrees is not associated with any increase in electricity consumption. An increase of temperature from 27 degrees (Celsius) to 28 degrees increases electricity consumption by 3%; and an increase of temperature from 30 degrees (Celsius) to 32 degrees increases electricity consumption by 6%. The number of annual hours with average temperatures above 30 degrees (Celsius) is expected to double between 2020 and 2050, from an equivalent of 10 days to 20 days. According to these estimates, global warming would at most explain a doubling of the energy-saving premium by 2050.

D Tree canopy and pollution

This section describes the data underlying Panel C of Table 5 and provides additional empirical analyses of the pollution-abatement effect of trees.

Figure D1. PM2.5 concentration in July 2007.

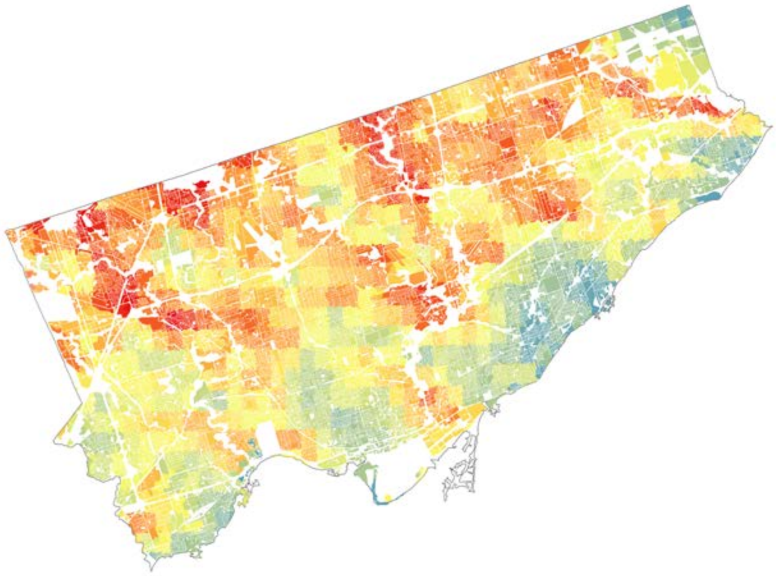

Notes: This Figure displays the PM2.5 concentration as recorded in July 2007 and nested at the level of postal codes. The color scale goes from light blue to red (corresponding to equal intervals of pollution between 9 $\mu g/m^3$ to 13 $\mu g/m^3$). The data is based on Aerosol Optical Depth (AOD) measures from NASA MODIS (250m horizontal resolution), NASA MISR (about 1.1 km horizontal resolution), and NASA SeaWIFS (to cover the oceans). Source: Van Donkelaar et al. (2021), and CANUE.

D.1 Data sources

We rely on monthly estimates of fine particulate matter (PM2.5) provided by Van Donkelaar et al. (2021) for the period 1998–2021.[20] The data is based on Aerosol Optical Depth (AOD) measures from NASA MODIS (250m horizontal resolution), NASA MISR (about 1.1 km horizontal resolution), and NASA SeaWIFS (to cover the oceans). These satellite-based measures are combined with a dispersion model (i.e., the GEOS-Chem chemical transport model, see Van Donkelaar et al., 2021), which is calibrated using a subsample of ground-based observations.

The main input (and constraint on spatial resolution) is the Aerosol Optical Depth (AOD) from MODIS, inducing a coarser spatial resolution than in our other

[20] The data is available on the CANUE website. Acknowledgments: PM2.5 metrics, indexed to DMTI Spatial Inc. postal codes , were provided by CANUE (Canadian Urban Environmental Health Research Consortium).

satellite-based measures. We illustrate the resulting variation in fine particulate matter nested across postal codes in Figure D1, where we display PM2.5 concentration in July 2007. One can see that there is still significant local variation, partly explained by the location of the main entry/exit points to/from the city—the Don Valley Parkway in the center of the map, Toronto Pearson airport (West), or the King's Highway 401. One corollary is that there might exist a spurious correlation between urban forestry (e.g., along the Don Valley) and air pollution. Our empirical strategy arguably addresses this issue.

Figure D2. Pollution concentration over time.

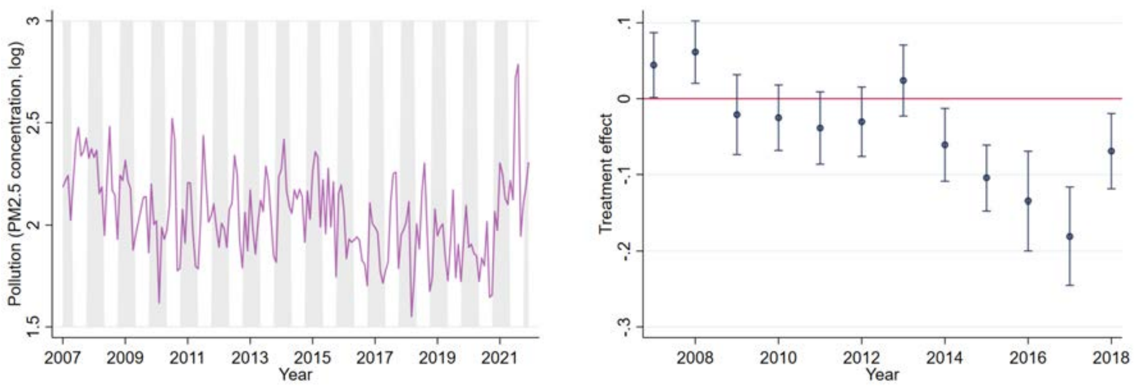

(a) Evolution over time

(b) Treatment effect

Notes: The left panel of the graph shows the monthly concentration of small particles (PM2.5, in $\mu g/m^3$) across postcodes in Toronto. The right panel shows the estimated correlation between tree density and (log) pollution for the months of July and August for each year between 2007 and 2018 (in a specification akin to Equation 4). More specifically, we regress (log) pollution across postcodes on the measure of tree cover in 2018, instrumented by the number of street ash trees per area within a 10m buffer (as measured in 2010). We control for a measure of street tree density, ward fixed effects, latitude, longitude, and dummies for the land classification in 2007 (tree canopy, grass/shrub, bare earth, water, buildings, roads, other paved surfaces and agriculture). The reported coefficients are the ones in front of the measure of tree density, and vertical lines show 95 percent confidence intervals.

Panel (a) of Figure D2 illustrates seasonal and more secular variations in the concentration of fine particulate matter across the City of Toronto. The series is quite volatile and exhibits irregular seasonal patterns: pollution peaks are more frequent in summer, but a few occur in winter as well. There is no academic consensus about the local pollution-abatement effect of a tree canopy (and its variation across seasons). Indeed, foliage prevents the dispersion of vehicle emissions (especially in road canyons, e.g., along the Don Valley Parkway), but increases the concentration of pollutants below the tree canopy (see, e.g., Salmond et al., 2013; Jin et al., 2014). We investigate these effects within our context in the next section.

D.2 The pollution-abatement effect of trees

The pollution-abatement effect of trees (during summer) We investigate the impact of trees on air pollution in a specification akin to Equation (3), i.e., we estimate,

$$\ln(P_{pt}) = \alpha + \beta TD_{pt} + \gamma_t \mathbf{X}_p + \eta_p + \mu_t + \varepsilon_{pt}, \tag{7}$$

where each observation is a postal code in a given year, P_{pt} is the average concentration of fine particulate matter within postcode p during July and August of that year, and urban forestry, TD_{pt}, is instrumented by the density of ash trees, A_{pt}. Controls include postcode fixed effects, latitude and longitude interacted with time fixed effects, the density of publicly maintained trees interacted with time fixed effects, and area shares from the land classification in 2007, interacted with year fixed effects.

We reported the estimates from Equation (7) in Panel C of Table 5. We find a negligible, yet negative, correlation in column (1). The causal estimate, reported in column (2), is negative as well, but one order of magnitude larger: a one percentage point increase in the area share of tree cover reduces the estimated PM2.5 concentration by 0.12% during the months of July and August. This effect is statistically significant, but remains quite small: postal codes that were most affected by the ecological catastrophe lost 0.07 in tree cover, leading to a drop in pollution of 0.84%.

The pollution-abatement effect of trees over time We replicate the exercises discussed in Figures C1 and C2 (see Equation 4) to shed light on the dynamic impact of the ecological catastrophe. We report the year-specific estimates in Panel (b) of Figure D2; we see that the pollution-abatement effect of trees materializes between 2013 and 2016—the period in which city-managed ash trees were removed.

The pollution-abatement effect of trees (during winter) We finally conduct a placebo exercise in Table D1, in which we replicate Panel C of Table 5 with PM2.5 concentration *during winter* (December-February) as the dependent variable. Both the OLS and the IV specifications provide negligible estimates, non-statistically significant for the latter. The absence of foliage indeed limits the impact of a tree canopy, whether positive or negative (Salmond et al., 2013; Jin et al., 2014).

Table D1. The pollution-abatement effect of trees—a placebo.

Pollution (PM2.5)	(1)	(2)
Tree cover	0.0010	-0.0018
	(0.0002)	(0.0036)
Observations	373,610	373,610
F-statistic	-	548.50

Notes: Robust standard errors are reported between parentheses. The unit of observation is a postcode. Across both panels, column (1) reports the OLS estimate while column (2) reports the estimates from an IV specification where tree cover is instrumented by a measure of ash tree density. All specifications include: latitude and longitude; the density of publicly maintained trees; and area shares from the land classification in 2007, all interacted with year fixed effects. The dependent variable is (log) concentration of PM2.5 in December-February (in $\mu g/m^3$), and we control for postcode fixed effects.